3D Level Set-FEM Techniques for (non-Newtonian) Multiphase Flow Problems

Benchmarking and Applications to Monodisperse Droplet Generation and Micro-Encapsulation

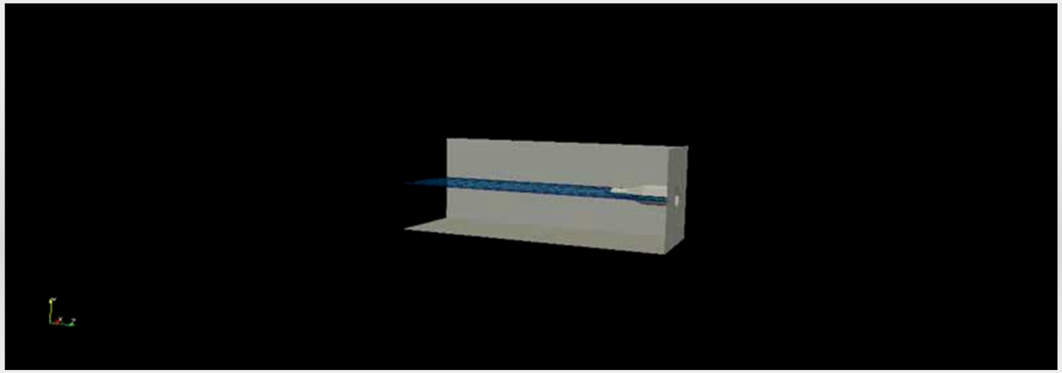

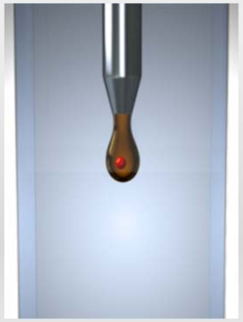

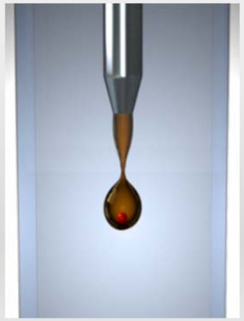

S. Turek, H. Damanik, O. Mierka, R. Münster
Institut für Angewandte Mathematik, LS III
Technische Universität Dortmund
ture@featflow.de

http://www.mathematik.tu-dortmund.de/LS3
http://www.featflow.de

Motivation: Fluid Prilling and Encapsulation

- Numerical simulation of *micro-fluidic drug encapsulation ("monodisperse compound droplets")*
- Polymeric "bio-degradable" outer fluid with generalized Newtonian/viscoelastic behaviour
- Optimization/Optimal control w.r.t. boundary conditions, flow rates, droplet size, geometry

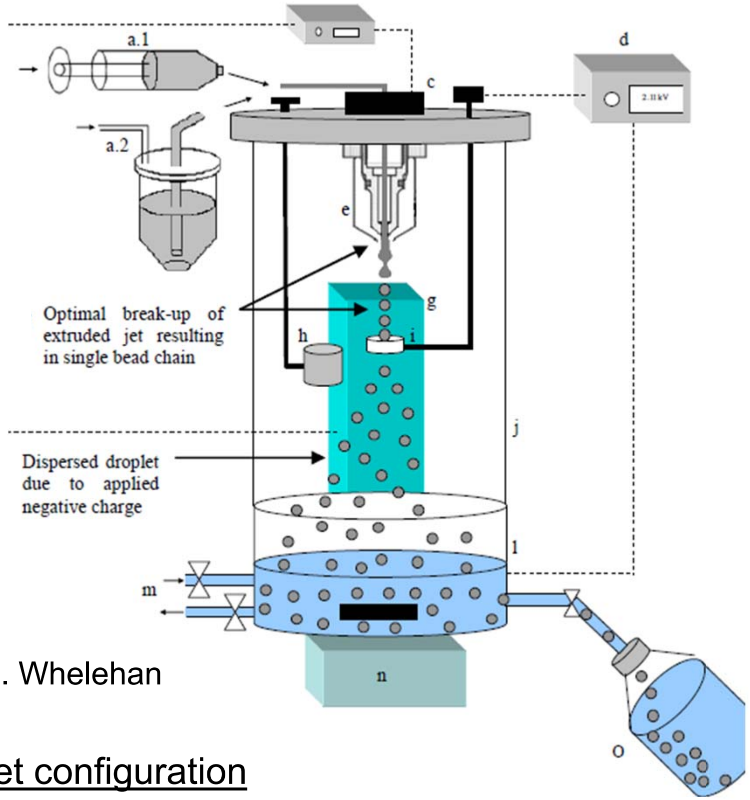

M. Whelehan

In Pharmaceutics

- Controlled drug release
- Protection of chemically active ingredients (from both sides)
- Protection against shear stress in stirred reactors
- Protection against evaporation
- Taste or odor masking

Jet configuration

- Core material is defined as the specific material that requires to be coated (liquid, emulsion, colloid or solid)
- Shell material is present to protect and stabilize the core (Alginate, Chitosan, Gelatin, Pectin, Waxes, Starch)

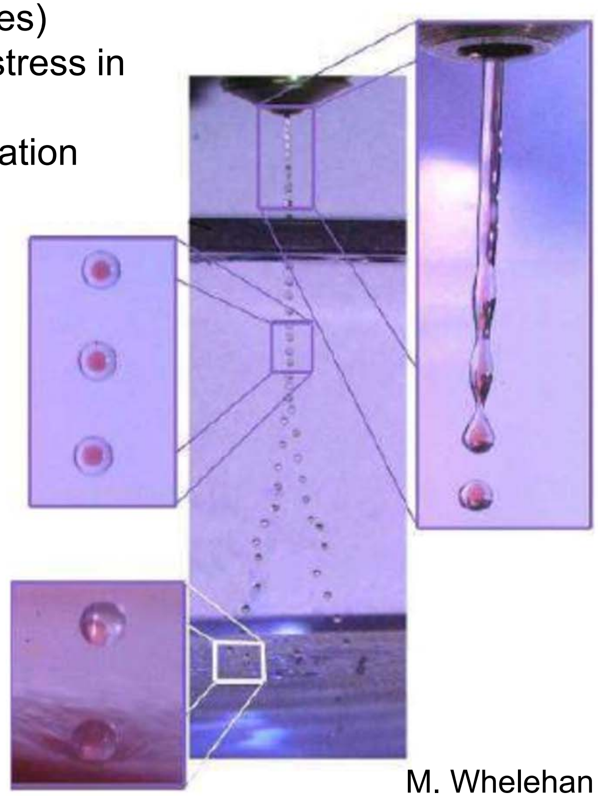

M. Whelehan

Motivation: Fluid Prilling and Encapsulation

	Tasks related to code development	Tasks related to application
mgLS-FBM-FEM flow module	• Multiple Level Set fields for simulation of liquid core encapsulation - l/l/g • Fictitious boundary method for particle encapsulation - s/l/g	• Validation via experimental results • Modulation for monodisperse compound drops

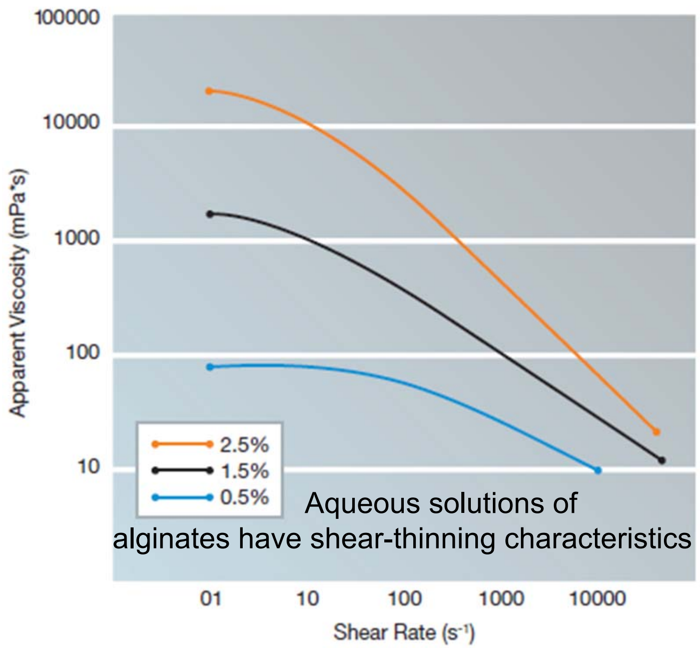

Preliminary simulation results for encapsulation of solid particles

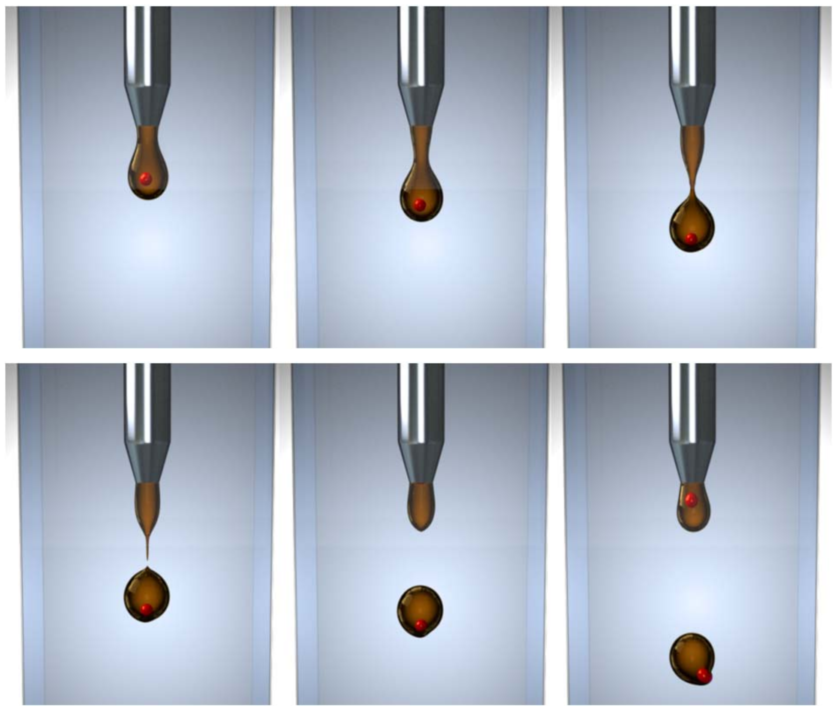

Modular Structure of mgLS-FBM-FEM

Basic flow solver – **FEATFLOW**
(robust, parallel, efficient)

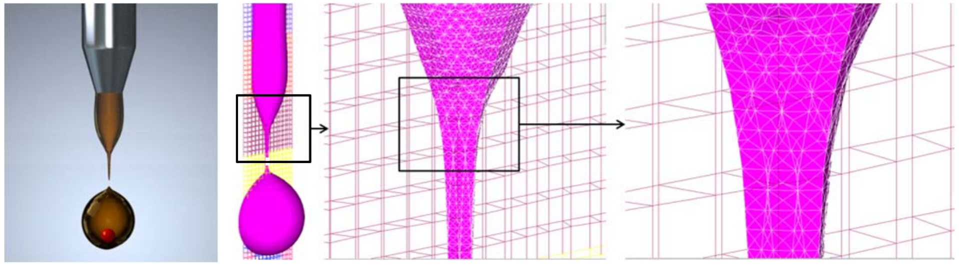

Numerical features:
- Higher order Q2P1 FEM schemes
- FCT & EO FEM stabilization techniques
- Use of unstructured meshes
- Fictitious Boundary (FBM) methods
- Dynamic adaptive grid deformation
- Newton-Multigrid solvers

Non-Newtonian flow module:
- generalized Newtonian model (Power-law, Carreau, ... etc.)
- viscoelastic model (Giesekus, Oldroyd B, …etc.)

Multiphase flow module (resolved interfaces):
- ℓ/ℓ – interface tracking method (levelset)
- s/ℓ – interface capturing method (FBM)
- $s/\ell/\ell$ – combination of ℓ/ℓ and s/ℓ

Engineering aspects:
- Geometrical design
- Modulation strategy
- Optimization

FEM-based simulation tool for the accurate prediction of „tailor-made“ droplet generation within encapsulation processes

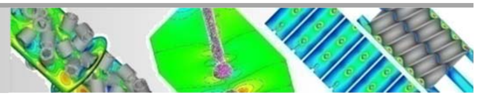

I) Treatment of Reinitialization

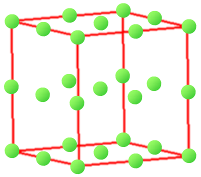

Higher order Q2 discretization of the Level Set equation $\frac{\partial \phi}{\partial t} + \mathbf{v} \cdot \nabla \phi = 0$

Stability requirement: ϕ should be smooth! → Stabilization for transport?

Reinitialization / Accurate distance computation / Interface reconstruction

- Triangulation of the arising surface

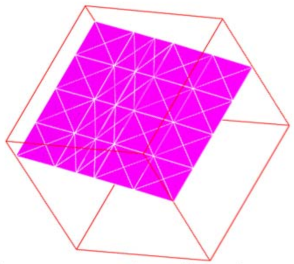

- Recursive subdivision of interface intersected elements (downward direction)

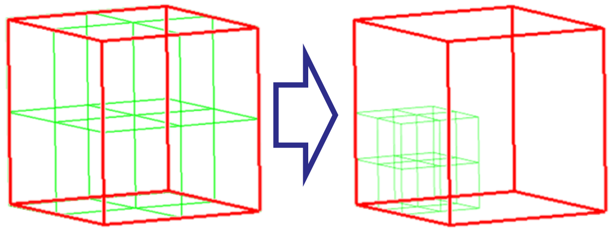

- Hierarchical storage of triangulated subsets (upward direction)

Reduction to mass of points weighted with their integral area

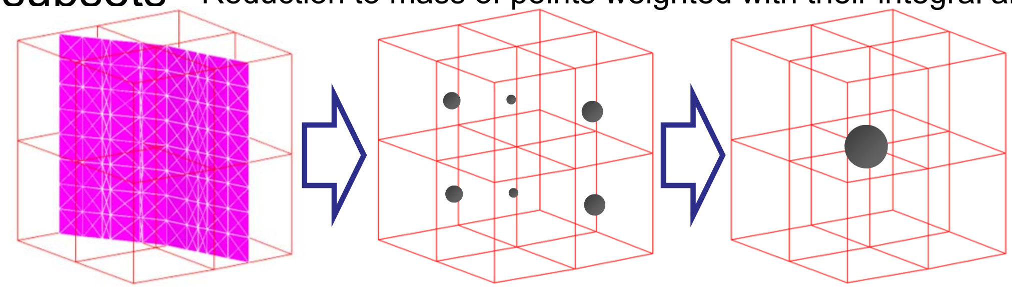

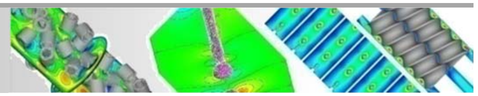

Practical Realization – Interface Reconstruction

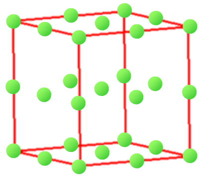

Higher order Q2 discretization of the Level Set equation $\frac{\partial \phi}{\partial t} + \mathbf{v} \cdot \nabla \phi = 0$

Stability requirement: ϕ should be smooth! → Stabilization for transport?

Reinitialization / Accurate distance computation / Interface reconstruction

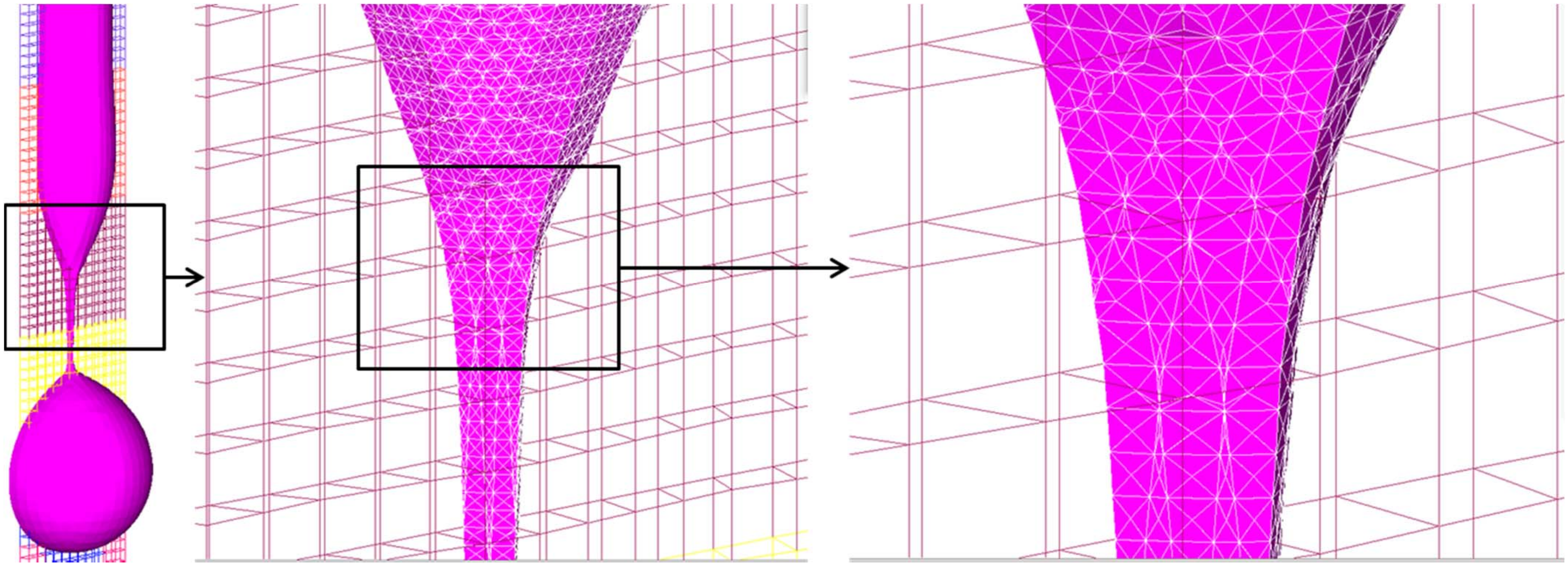

Practical Realization – Reinitialization

General experience related to reinitialization with respect to nodal dof's:

- Artificial interface movement due to reinitialization $\xrightarrow[\text{reinitailization}]{\text{Intensive use of}}$ Systematic translation, Mass loss
- Steep or flat gradients of the Level Set function $\xrightarrow[\text{reinitailization}]{\text{Rare use of}}$ Numerical oscillation, Mass loss

Other alternative is the use of
- multiple fields: 1) indicator field ϕ
  2) exact distance field $\tilde{\phi}$
- the use of L2 projection $$\int \tilde{\phi} w \, dx = \int \text{dist } w \, dx$$

$$\phi := M_L^{-1} \int (\alpha_{\text{reini}} \text{dist} + (1 - \alpha_{\text{reini}})\phi) \, w \, dx$$

Next aims: Choose locally adaptive weighting parameter
Avoid explicit reconstruction for calculating dist(x)

Q2 element

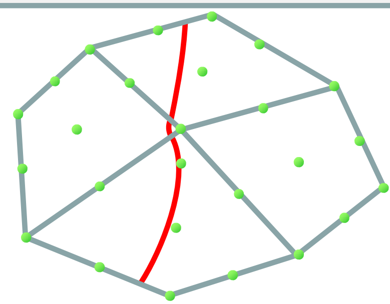

Estimation of shortest distances against dof's

3x3 Gauss formula

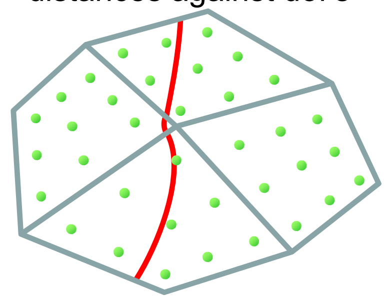

Estimation of shortest distances against integration points

Treatment of Surface Tension

<u>Surface Tension</u>: Semi-implicit CSF formulation based on Laplace-Beltrami

$$\mathbf{f}_{ST} = \int_\Omega \sigma\kappa\hat{\mathbf{n}}\cdot\mathbf{v}\,\delta(\Gamma,\mathbf{x})\,d\mathbf{x} \quad = \int_\Omega \sigma\left(\underline{\Delta}\mathbf{x}|_\Gamma\right)\cdot\left(\mathbf{v}\,\delta(\Gamma,\mathbf{x})\right)d\mathbf{x}$$

$$= -\int_\Omega \sigma\underline{\nabla}\mathbf{x}|_\Gamma\cdot\underline{\nabla}\left(\mathbf{v}\,\delta(\Gamma,\mathbf{x})\right)d\mathbf{x} = -\int_\Omega \sigma\underline{\nabla}\mathbf{x}|_\Gamma\cdot\underline{\nabla}\mathbf{v}\,\delta(\Gamma,\mathbf{x})\,d\mathbf{x}$$

Application of the semi-implicit time integration yields $\mathbf{x}|_{\Gamma^{n+1}} = \mathbf{x}|_{\Gamma^n} + \Delta t\,\mathbf{u}^{n+1}$

$$\Downarrow$$

$$\mathbf{f}_{ST} = -\int_\Omega \sigma\,\delta_\varepsilon\left(dist(\Gamma^n,\mathbf{x})\right)\underline{\nabla}\tilde{\mathbf{x}}|_\Gamma^n\cdot\underline{\nabla}\mathbf{v}\,d\mathbf{x}$$

$$-\Delta t^{n+1}\int_\Omega \sigma\,\delta_\varepsilon\left(dist(\Gamma^n,\mathbf{x})\right)\underline{\nabla}\mathbf{u}^{n+1}\cdot\underline{\nabla}\mathbf{v}\,d\mathbf{x}$$

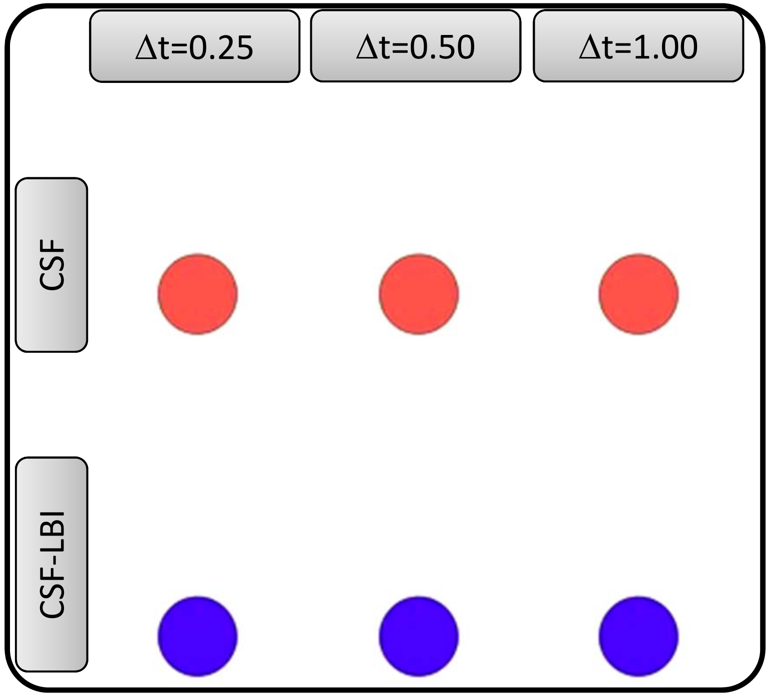

Advantages
- Relaxes *Capillary Time Step* restriction
- „Optimal“ for FEM-Level Set approach due to global information

Aim: Curvature-free Surface Tension

- Standard surface tension approach

$$\left(\frac{\partial \mathbf{u}}{\partial t} + u \cdot \nabla \mathbf{u}\right) - \operatorname{div} \boldsymbol{\tau} + \nabla p = \rho \mathbf{f} + \mathbf{f}_{\mathrm{CSF},1}$$

$$\mathbf{f}_{\mathrm{CSF},1} = \kappa \sigma \mathbf{n} \delta_\Gamma$$

- Curvature-free surface tension

$$\psi = \frac{1}{1 + e^{\frac{\mathrm{dist}_\Gamma}{\epsilon}}} \qquad \mathbf{n}\delta_\Gamma = \nabla \psi \qquad \kappa = -\nabla \cdot \mathbf{n} \qquad \mathbf{n} = \frac{\nabla \psi}{\|\nabla \psi\|}$$

$$\mathbf{f}_{\mathrm{CSF},2} = -\sigma \nabla \cdot \left(\frac{\nabla \psi}{\|\nabla \psi\|}\right) \nabla \psi$$

$$\mathbf{f}_{\mathrm{CSF},3} = -\sigma \nabla \cdot \left(\frac{\nabla \psi \otimes \nabla \psi}{\|\nabla \psi\|}\right)$$

Numerical Evaluation

2D Bubble Benchmarks

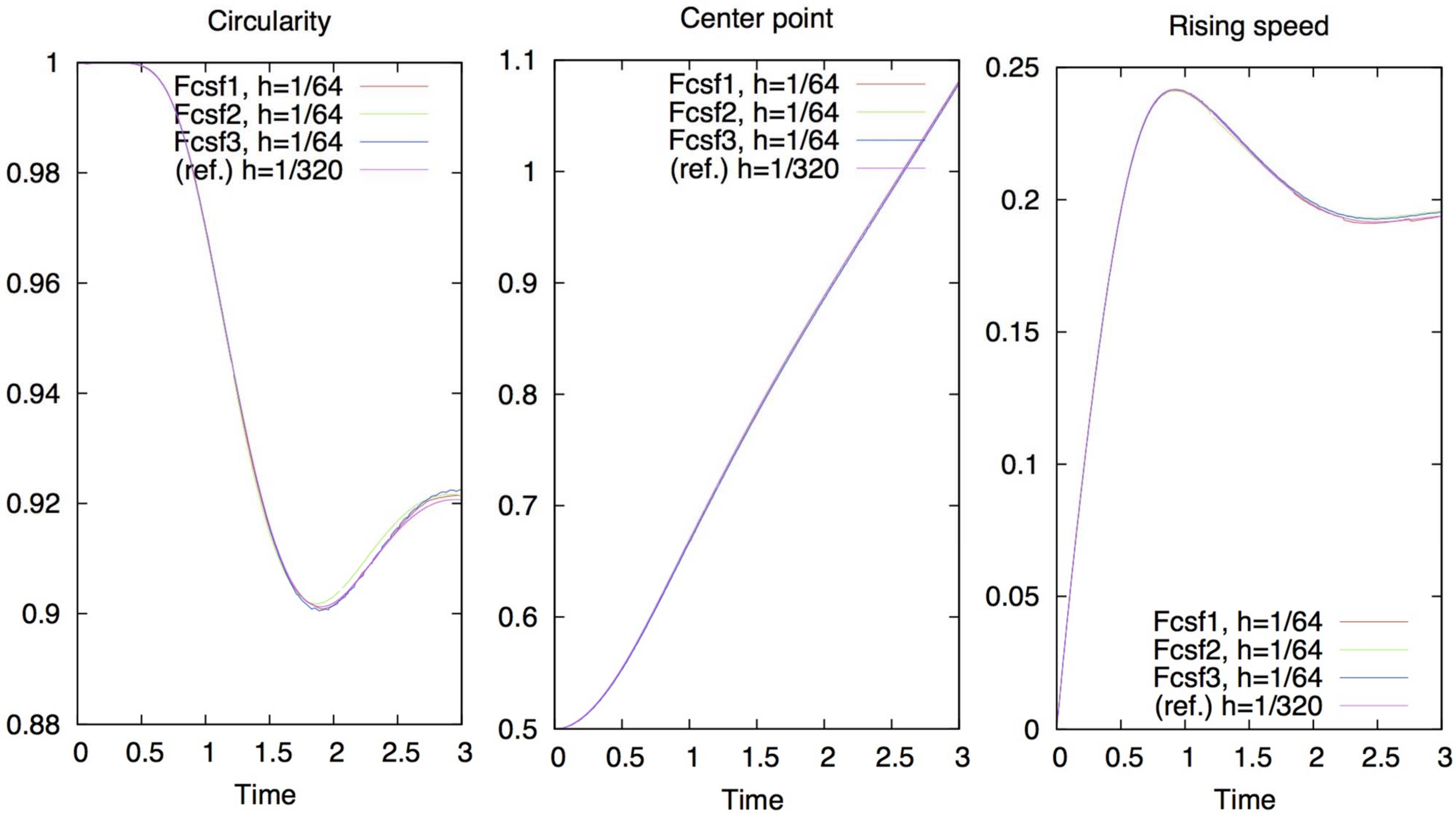

Towards a New Stress Formulation

$$\rho\left(\frac{\partial \mathbf{u}}{\partial t} + u \cdot \nabla \mathbf{u}\right) - \operatorname{div} \boldsymbol{\tau} + \nabla p = \rho \mathbf{f}$$

$$\boldsymbol{\tau} = \boldsymbol{\tau}_s + \boldsymbol{\tau}_{Xs}$$

$$\boldsymbol{\tau}_s = 2\mu \mathbf{D}(\mathbf{u})$$

$$\boldsymbol{\tau}_{Xs} = -\sigma\left(\frac{\nabla\psi \otimes \nabla\psi}{\|\nabla\psi\|}\right)$$

New stress, allowing more implicit coupling and more appropriate FEM spaces

Use of standard NSE solvers since no force term on right hand side

Validation of the 3D mgLS-FEM Flow Solver

3D rising Bubble

References:

- Annaland et al.,
- Clift and Grace

$$\boxed{\rho_1 : \rho_2 = \mu_1 : \mu_2 = 1:100}$$

$$\mathrm{Mo} = \frac{g_z \mu_l^4 \Delta\rho_{gl}}{\rho_l^2 \sigma_{gl}} \qquad \mathrm{Eo} = \frac{g_z \Delta\rho_{gl} d_b^2}{\sigma_{gl}}$$

$$\mathrm{Re} = \frac{\rho_l v_\infty d_b}{\mu_l}$$

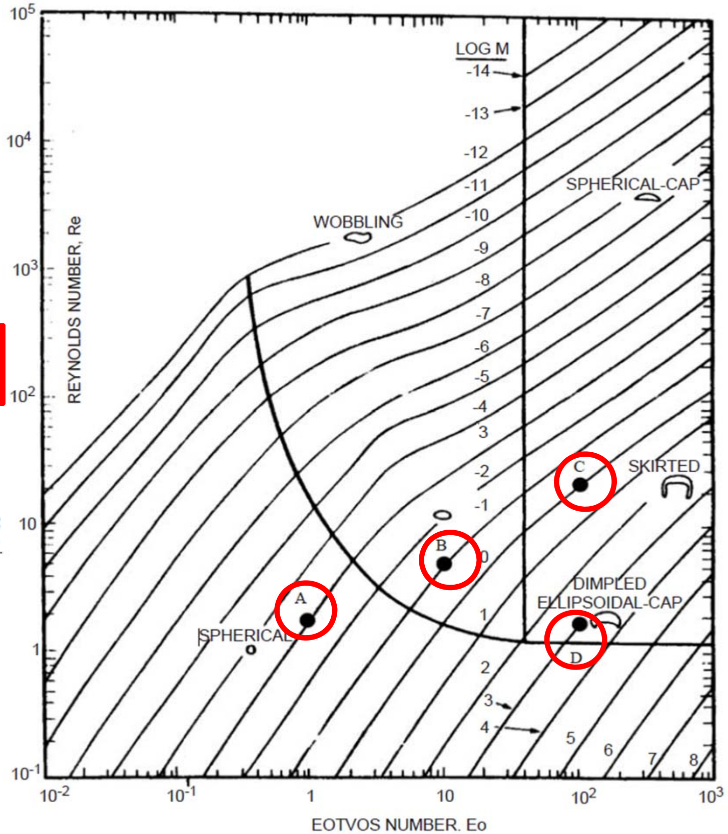

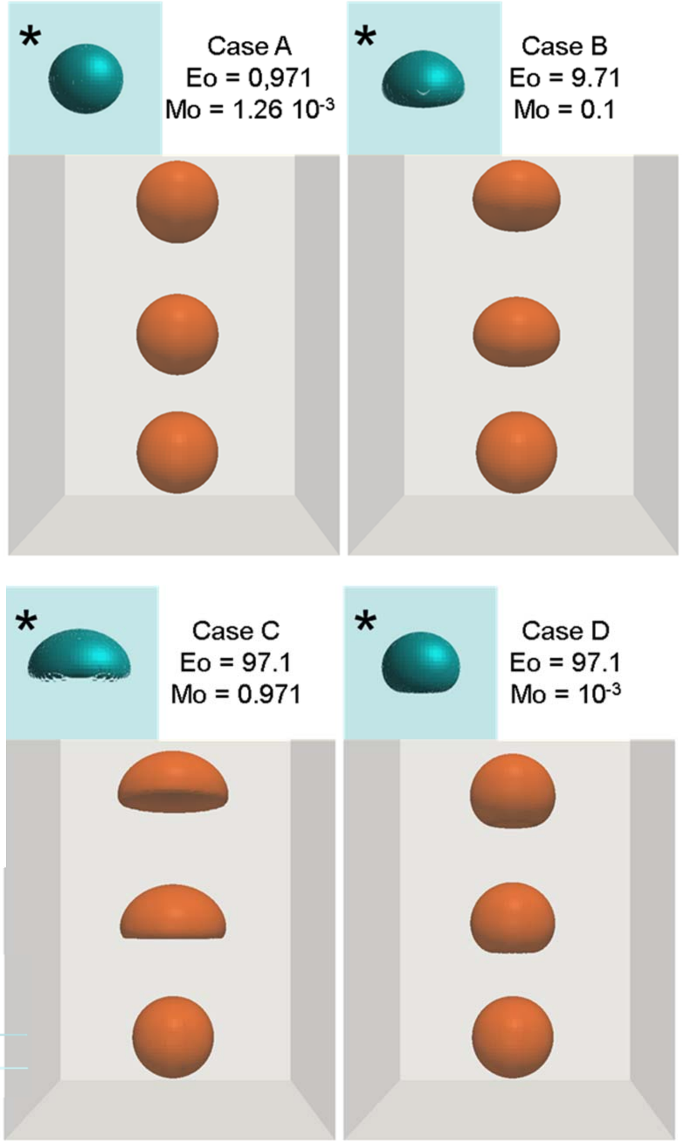

Case A	Case B	Case C	Case D
$\mathrm{Re}_{\mathrm{ExpRef}} = 1.7$	$\mathrm{Re}_{\mathrm{ExpRef}} = 4.6$	$\mathrm{Re}_{\mathrm{ExpRef}} = 20$	$\mathrm{Re}_{\mathrm{ExpRef}} = 1.5$
$\mathrm{Re}_{\mathrm{SimRef}} = 1.6$	$\mathrm{Re}_{\mathrm{SimRef}} = 4.3$	$\mathrm{Re}_{\mathrm{SimRef}} = 18$	$\mathrm{Re}_{\mathrm{SimRef}} = 1.7$
$\mathrm{Re}_{\mathrm{Sim}} = 1.57$	$\mathrm{Re}_{\mathrm{Sim}} = 4.39$	$\mathrm{Re}_{\mathrm{Sim}} = 17.2$	$\mathrm{Re}_{\mathrm{Sim}} = 1.58$

Benchmarking on Experimental Results

Group	Separation frequency [Hz]	Droplet size [dm]	Stream Length [dm]
BCI Dortmund	0,58	0,062	0,122
iRMB Braunschweig	0,37	0,068	0,113
AM&N Dortmund	0,60	0,058	0,102

Continuous phase:

Glucose-Water mixture

$$\mu_D = 500\, mPa\, s$$

$$\rho_D = 972\, kg\, m^{-3}$$

$$\dot{V}_D = 3{,}64\, ml\, min^{-1}$$

$$\boxed{\sigma_{CD} = 0{,}034\, N\, m^{-1}}$$

Silicon oil

$$\mu_C = 500\, mPa\, s$$

$$\rho_C = 1340\, kg\, m^{-3}$$

$$\dot{V}_C = 99{,}04\, ml min^{-1}$$

Dispersed phase:

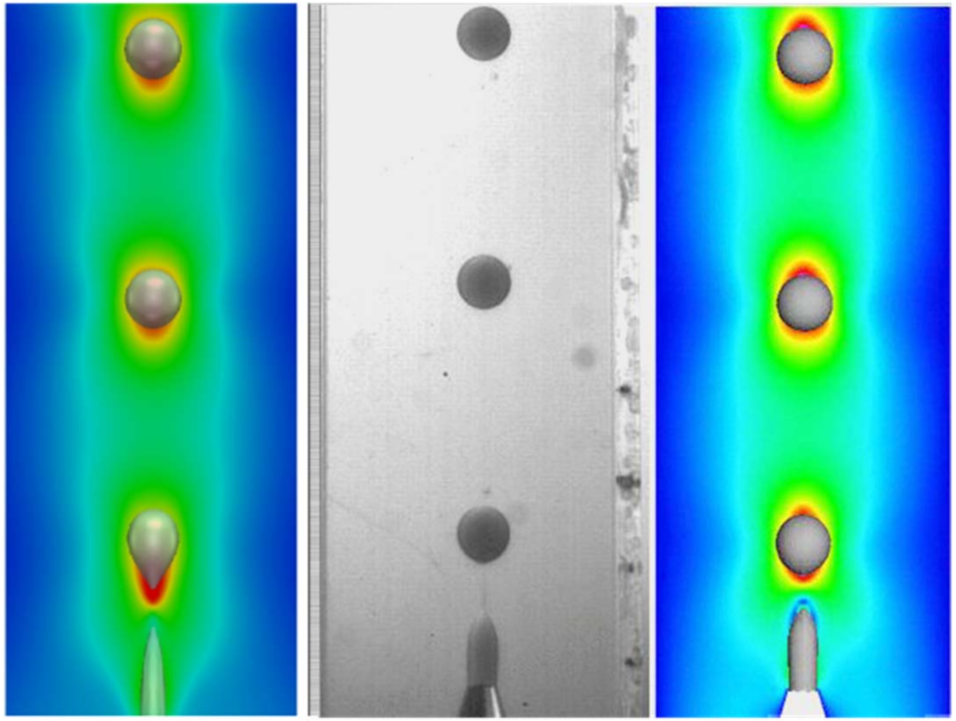

iRMB - LB   Exp   TU Do - FEM

Turek S., Mierka O., Hysing S., Kuzmin D.: *Numerical study of a high order 3D FEM-Level Set approach for immiscible flow simulation*, Repin, S., Tiihonen, T., Tuovinen, T., Numerical methods for differential equations, optimization, and technological problems, Springer, 2012.

Generalized Newtonian Flow Module - Validation

Single phase validation on 2D benchmark “flow around a cylinder”

Reference: Damanik et al.

	Shear thining n=0,75				Shear thickening n=1,50			
	Damanik*		Our results		Damanik*		Our results	
level	C_D	C_L	C_D	C_L	C_D	C_L	C_D	C_L
1	3,20082	-0,01261	3,20450	-0,01215	13,6209	0,34250	13,6233	0,34347
2	3,26433	-0,01342	3,26637	-0,01347	13,7380	0,35052	13,7379	0,35037
3	3,27739	-0,01342	3,27755	-0,01343	13,7688	0,34941	13,7688	0,34928

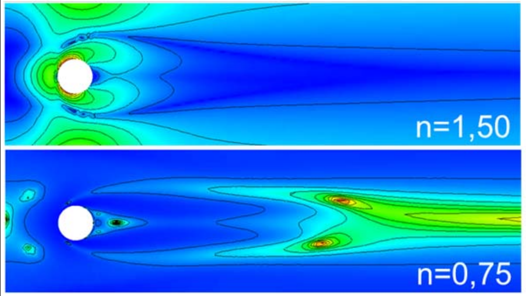

Viscosity distribution

Pseudo 2D rising bubble in Power-Law fluids

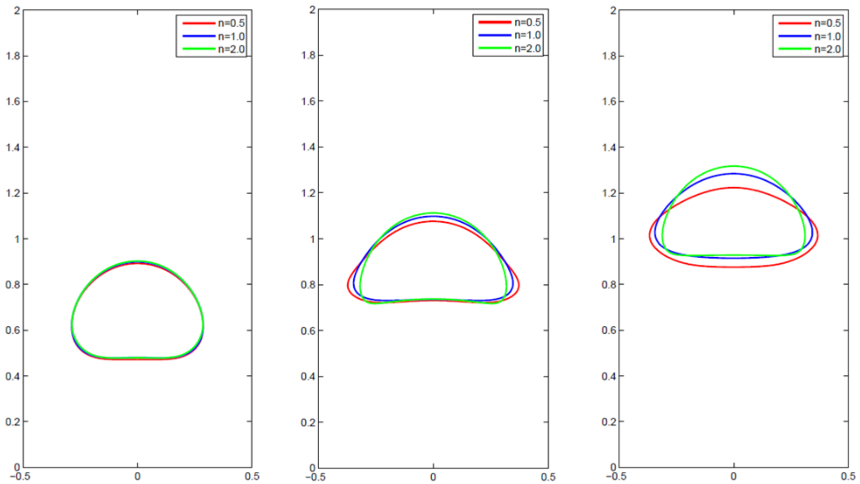

Mesh converged bubble shapes for n = 0.5, 1.0, 2.0

Droplet generation for Power-Law fluids

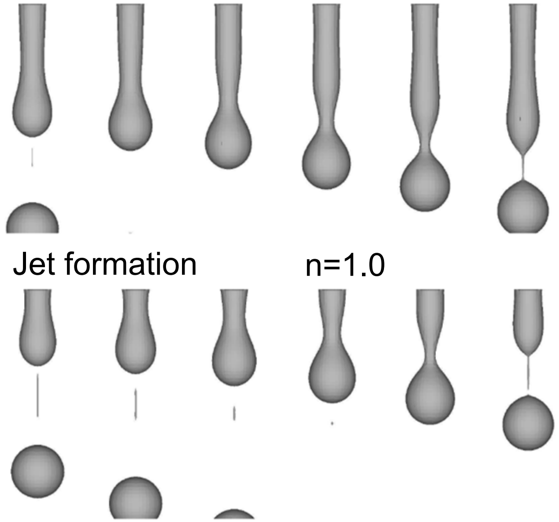
Jet formation n=1.0

Dripping n=0.5

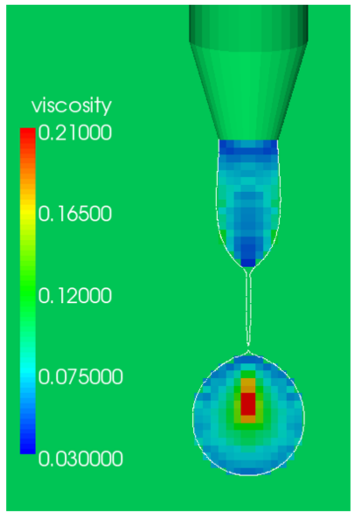

Instanteous viscosity distribution for n=0.5

Viscoelastic Multiphase Flow

Preliminary numerical results – 2D rising bubble

Material 1: Viscoelastic fluid described by the Oldroyd-B model

Material 2: Newtonian fluid

Test case	ρ_1	ρ_2	μ_1	μ_2	$\mathbf{g}$	σ
1. Viscoelastic ($\Lambda = 10$)	10	0.1	10	1	9.8	0.245
2. Newtonian ($\Lambda = 0$)	10	0.1	10	1	9.8	0.245
3. Viscoelastic ($\Lambda = 10$)	10	0.1	2	1	9.8	0.245
4. Newtonian ($\Lambda = 0$)	10	0.1	2	1	9.8	0.245

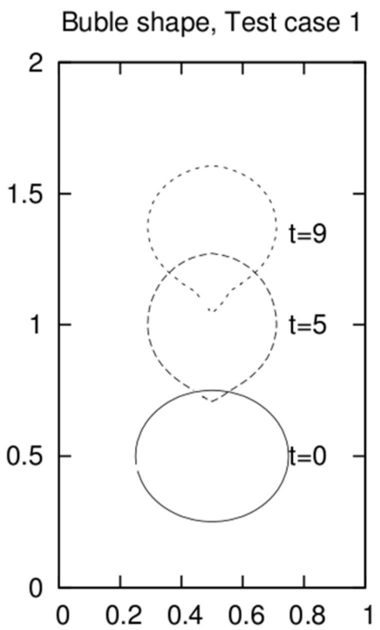

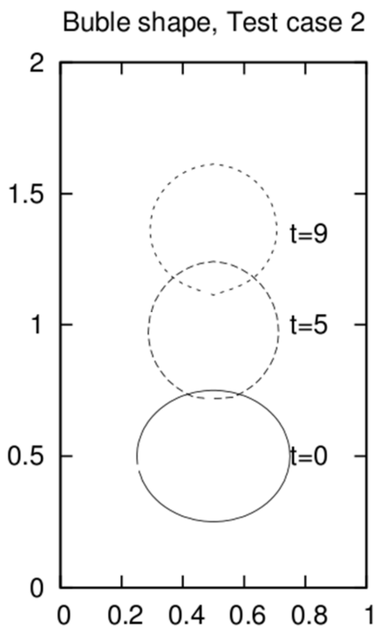

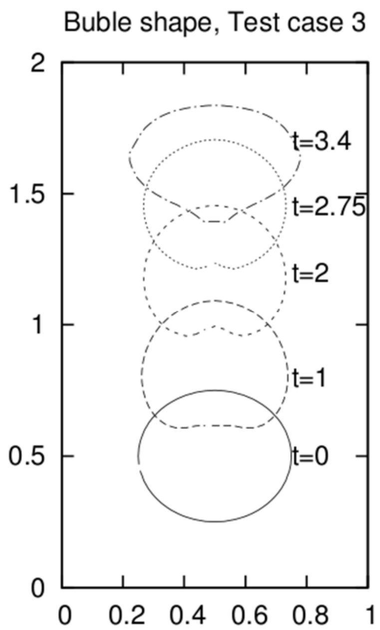

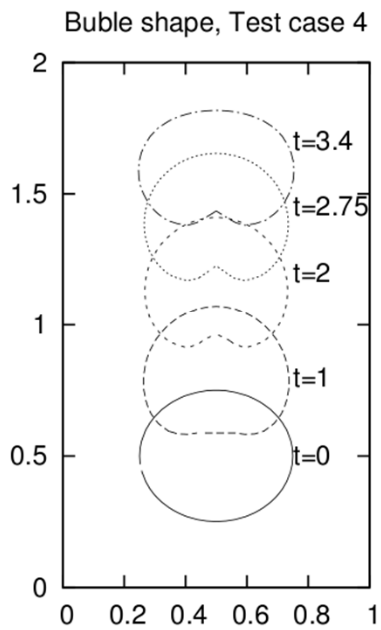

Next: Particulate Flow

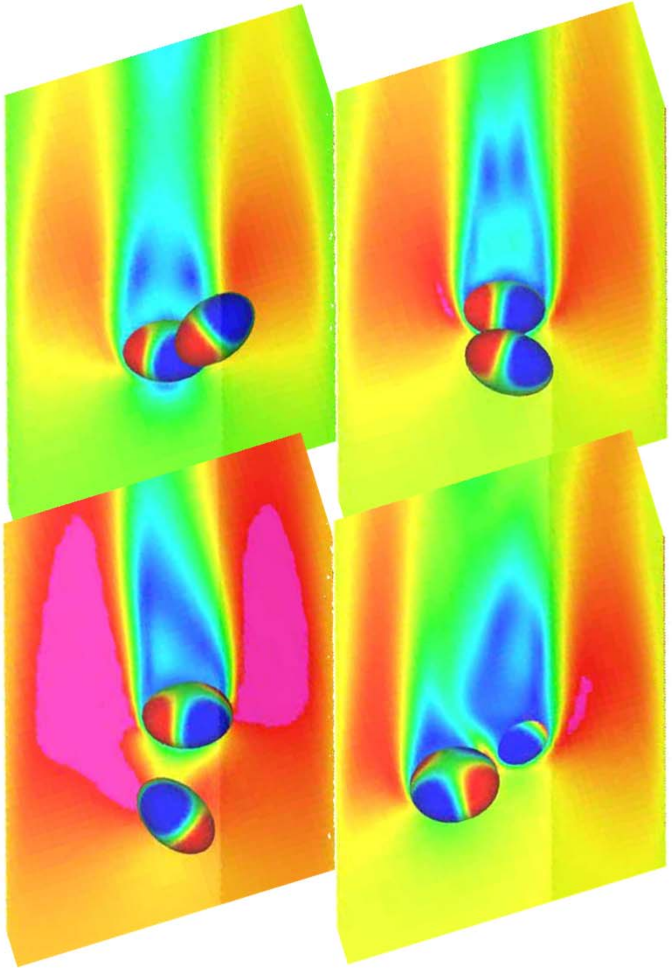

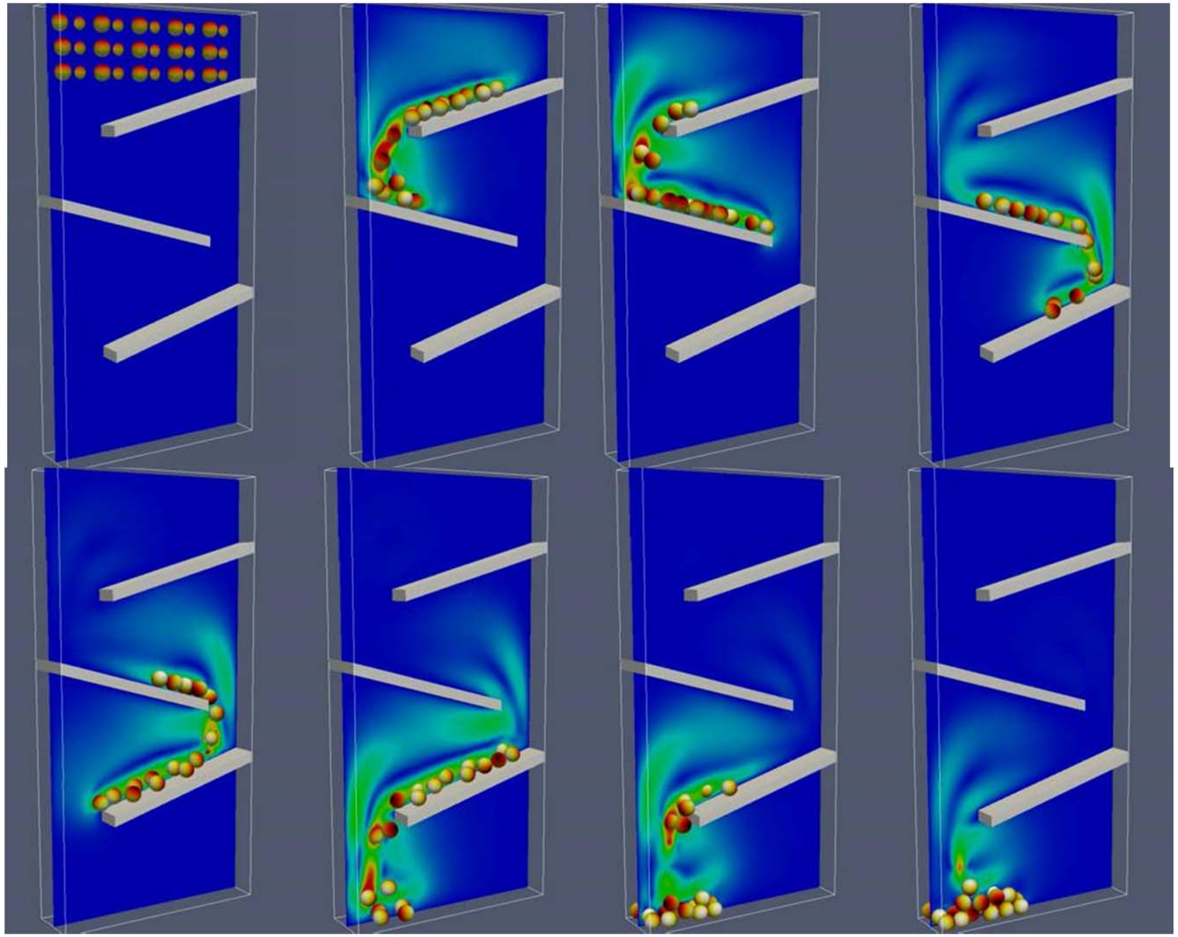

Modelling: Two-phase Flow (Solid-Liquid)

- **Fluid** motion is governed by the **Navier-Stokes equations**
- **Particle** motion is described by **Newton-Euler equations**

$$M_p \frac{dU_p}{dt} = F_p + F_{ex,col} + \left(\Delta M_p\right) g, \qquad I_p \frac{d\omega_p}{dt} = T_p - \omega_p \times \left(I_p \omega_p\right)$$

Hydrodynamic force

Torque

$$F_p = -\int_{\Gamma_p} \sigma \cdot n_p \, d\Gamma_p \quad \xleftrightarrow{\text{Postprocessing the actual flow field}} \quad T_p = -\int_{\Gamma_p} \left(X - X_p\right) \times \left(\sigma \cdot n_p\right) d\Gamma_p$$

Fictitious Boundary Method

- Surface integral is replaced by volume integral
- Use of monitor function (liquid/solid)

$$\alpha_p(X) = \begin{cases} 1 & \text{for} \quad X \in \Omega_p \\ 0 & \text{for} \quad X \in \Omega_f \end{cases}$$

- Normal to particle surface vector is non-zero only at the surface of particles $\quad n_p = \nabla \alpha_p$

$$F_p = -\int_{\Gamma_p} \sigma \cdot n_p \, d\Gamma_p = -\int_{\Omega_T} \sigma \cdot \nabla \alpha_p \, d\Omega_T$$

$$T_p = -\int_{\Gamma_p} \left(X - X_p\right) \times \left(\sigma \cdot n_p\right) d\Gamma_p = -\int_{\Omega_T} \left(X - X_p\right) \times \left(\sigma \cdot \nabla \alpha_P\right) d\Omega_T$$

Modelling: Two-phase Flow (Solid-Liquid)

Fictitious Boundary Method

For computed

$U_p^{n+1},\ \omega_p^{n+1}$

Position update: $\dfrac{dX_p}{dt} = U_p,$ Angle update: $\dfrac{d\theta_p}{dt} = \omega_p$

$X_p^{n+1},\ \theta_p^{n+1}$

Velocity "boundary condition" imposed for particles:

$$u(X) = U_p + \omega_p \times (X - X_p)$$

- supports HPC concepts (fixed data structures)
- easy grid generator
- relatively low resolution

  - Brute force → Finer mesh resolution
  - High resolution interpolation functions
  - **Grid deformation** (+ monitor function)

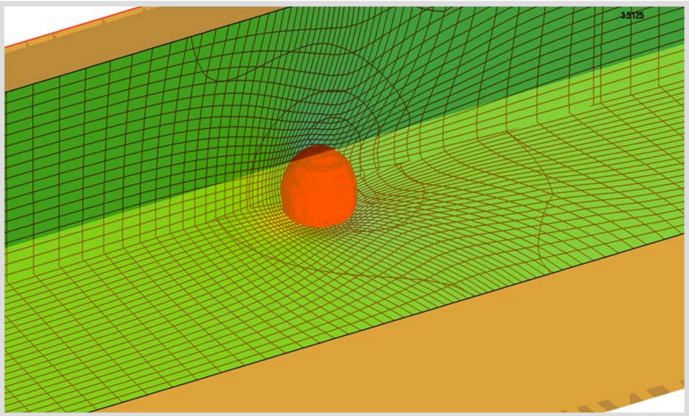

Adaptive Grid Deformation: Sedimentation of Particles

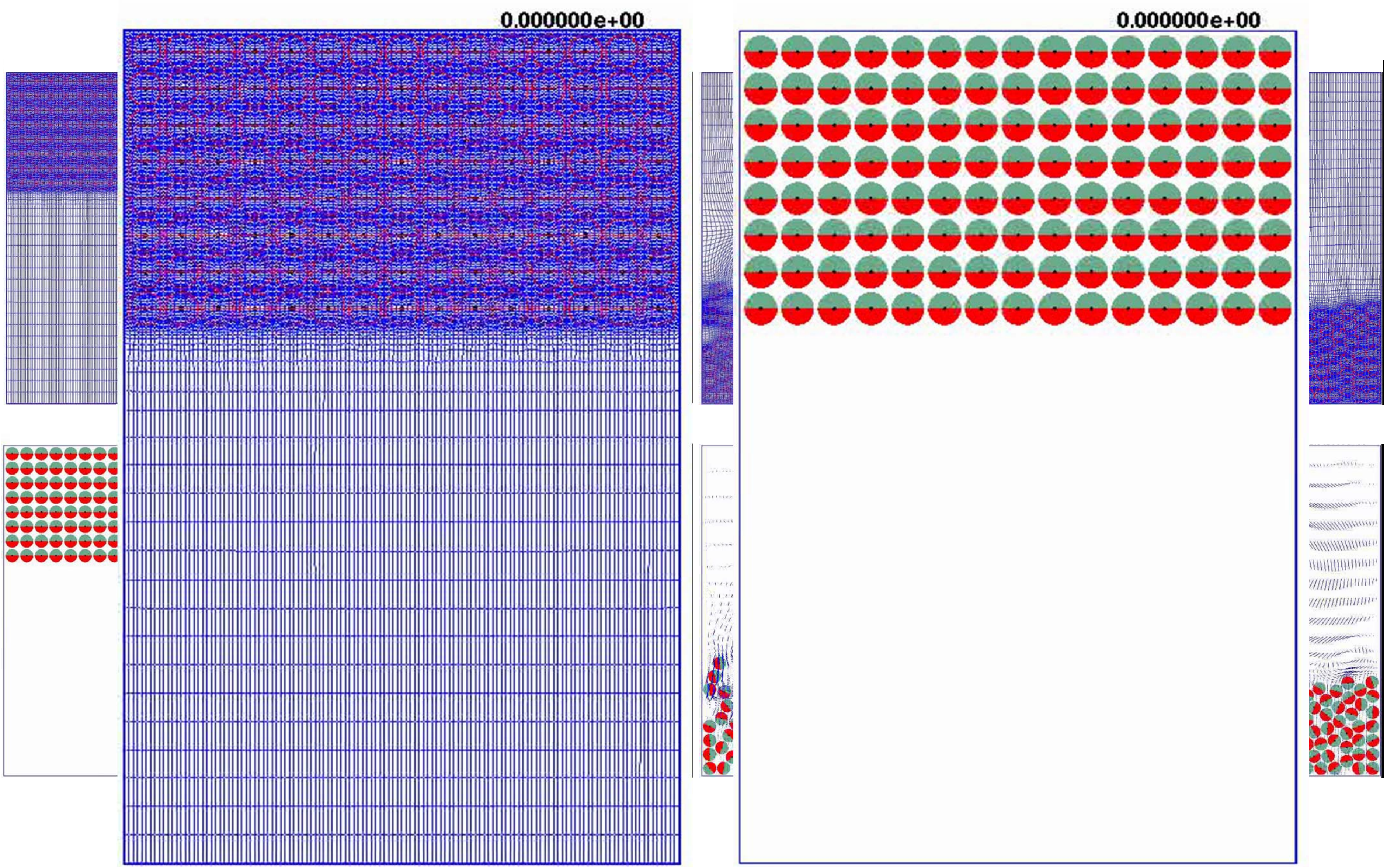

Numerical Solution Scheme

Solve for velocity and pressure applying FBM-conditions

$$NSE\left(u_f^{n+1}, p^{n+1}\right) = BC\left(\Omega_i^n, u_i^n\right)$$

Calculate hydrodynamic force, torque and apply

$$F_i^{n+1} \qquad T_i^{n+1}$$

Contact force calculation

$$F_{c,i}^{n+1}$$

Compute new velocity and angular velocity

$$u_i^{n+1} = u_i^n + \Delta t \left(F_{c,i}^{n+1} / M_i\right) \qquad \omega_i^{n+1} = \omega_i^n + \Delta t I_i^{-1}\left(r \times F_{c,i}\right)$$

Position update

$$X_i^{n+1} = X_i^n + \Delta t u_i^n \qquad \theta_i^{n+1} = \theta_i^n + \Delta t \omega_i^n$$

Benchmarking and Validation

Settling of a sphere towards a plane wall:
- Sedimentation Velocity
- Particle trajectory
- Kinetic Energy
- Different Reynolds numbers

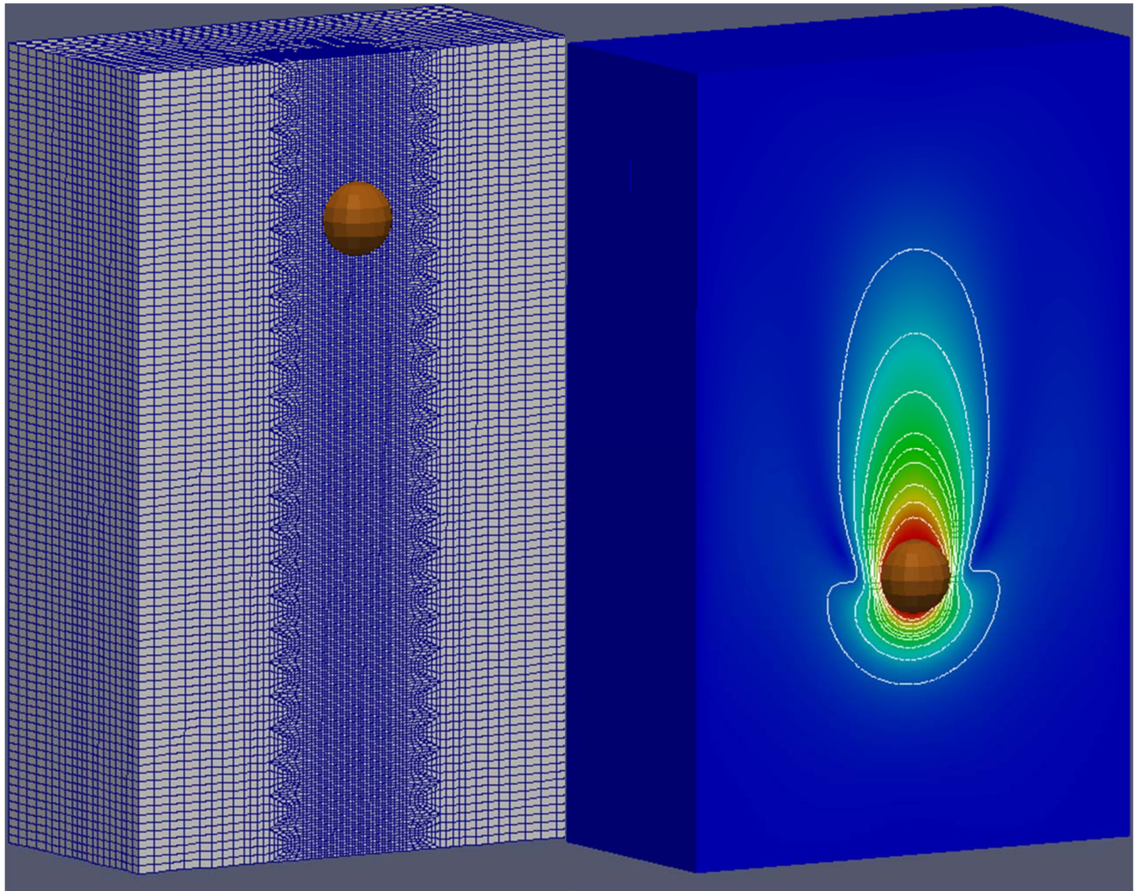

Setup

Computational mesh:
- 1.075.200 vertices
- 622.592 hexahedral cells
- Q2/P1:
  $\rightarrow$ 50.429.952 DoFs

Hardware Resources:
- 32 Processors

Benchmarking and Validation

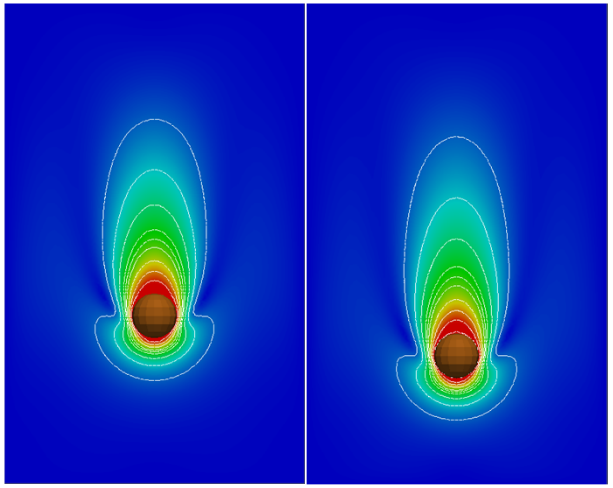

Observations

- Velocity profiles compare well to ten Cate's data
- Maximum velocity close to experiment
- Flow features are accurately resolved

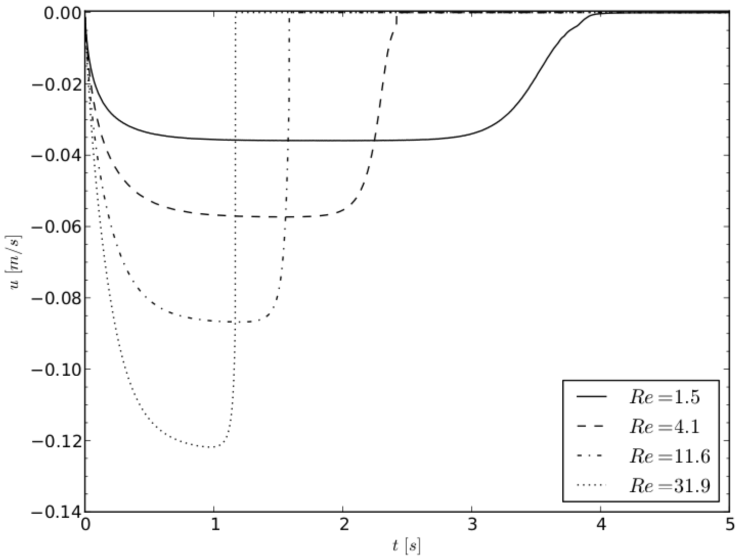

Re	u_{max}/u_∞	u_{max}/u_∞ *ten Cate*	u_{max}/u_∞ *exp*
1.5	0.945	0.894	0.947
4.1	0.955	0.950	0.953
11.6	0.953	0.955	0.959
31.9	0.951	0.947	0.955

Tab. 1 Comparison of the u_{max}/u_∞ ratios between the FEM-FBM, ten Cate's simulation and ten Cate's experiment

Benchmarking and Validation

Source: 13th Workshop on Two-Phase Flow Predictions 2012
Ernst,M., Dietzel,M., Sommerfeld,M.

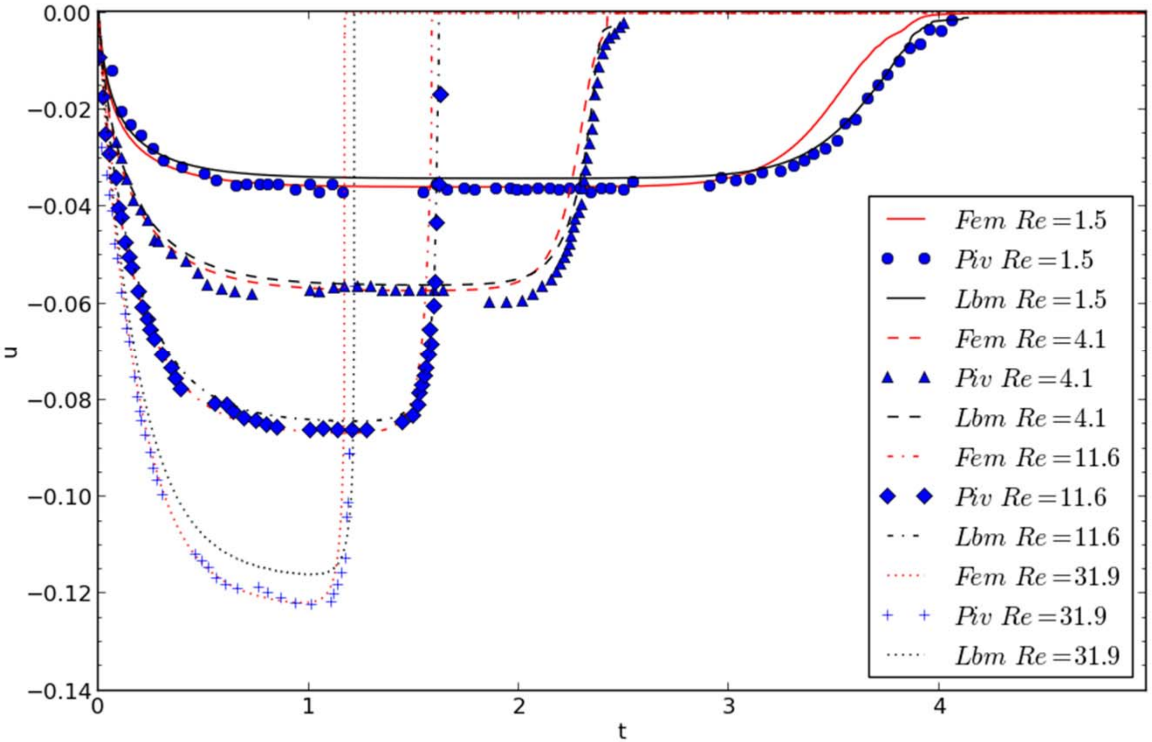

Comparison of FEM-FBM and the experimental values and the LBM results of the group of Sommerfeld

- *Increasing the mesh resolution produces more accurate results*
  Test performed at different mesh levels
  - Maximum velocity is approximated better ✓
  - Shape of the velocity curve matches better ✓

Complex Geometry Examples

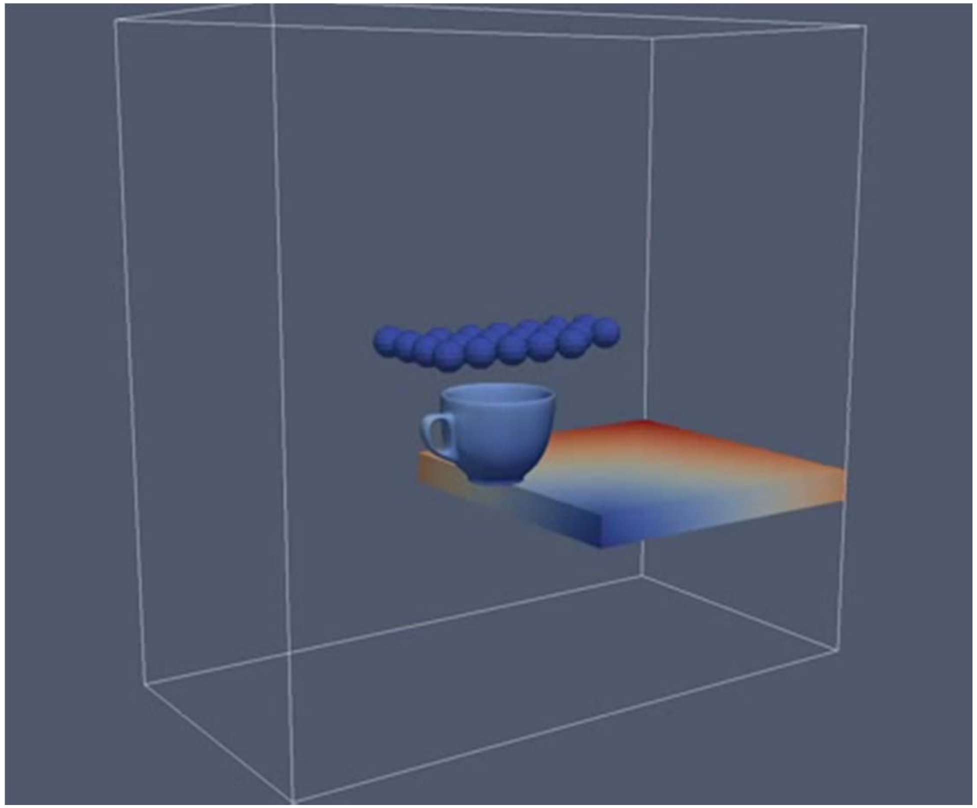

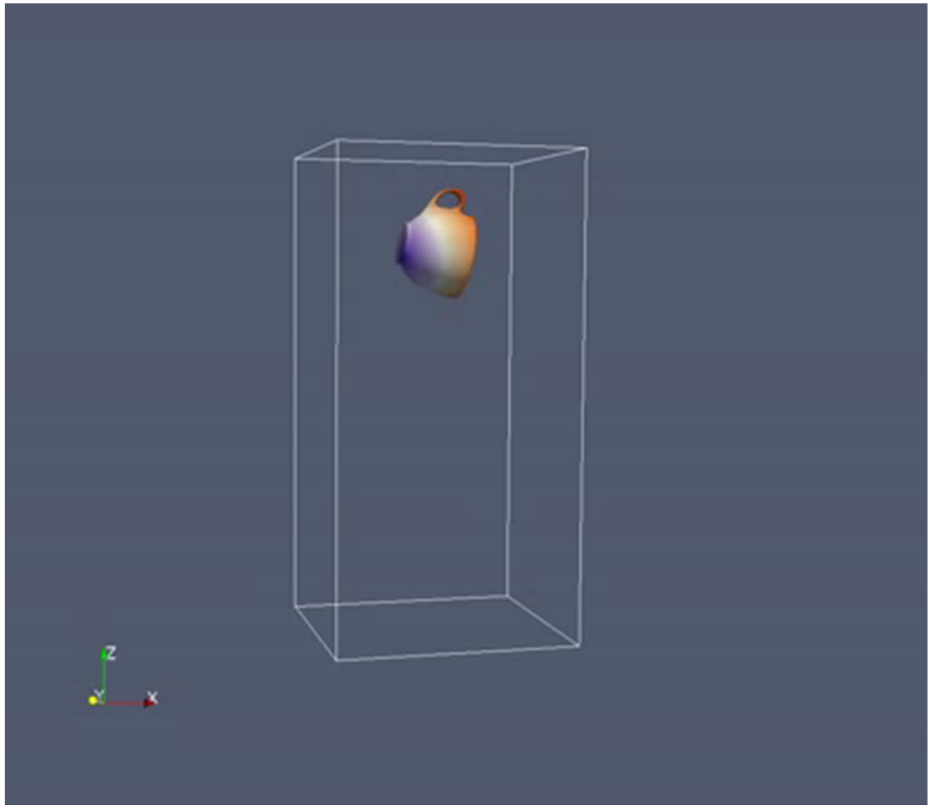

Fluidized Bed Example

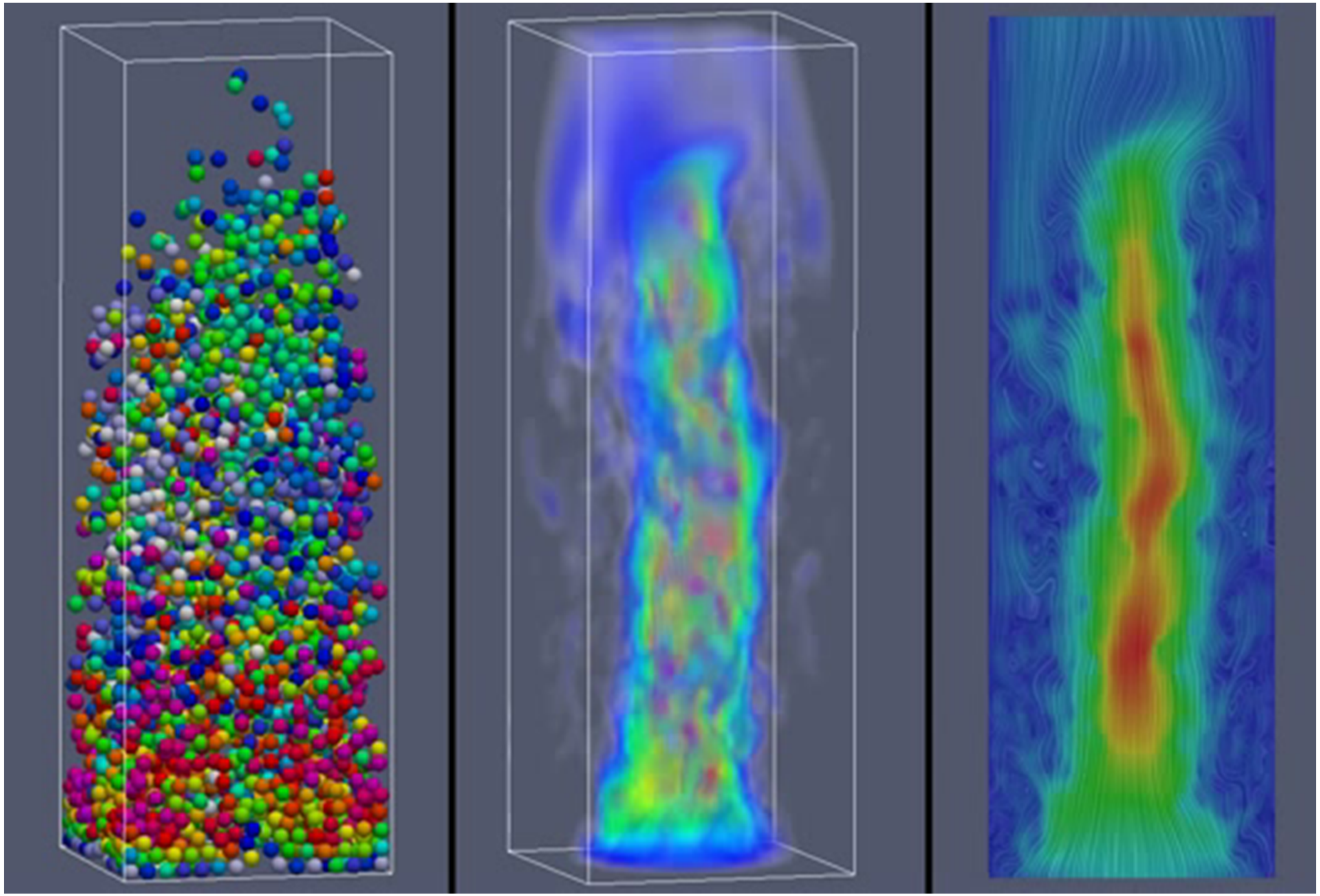

Bringing Everything Together: Preliminary Studies for Micro-Encapsulation

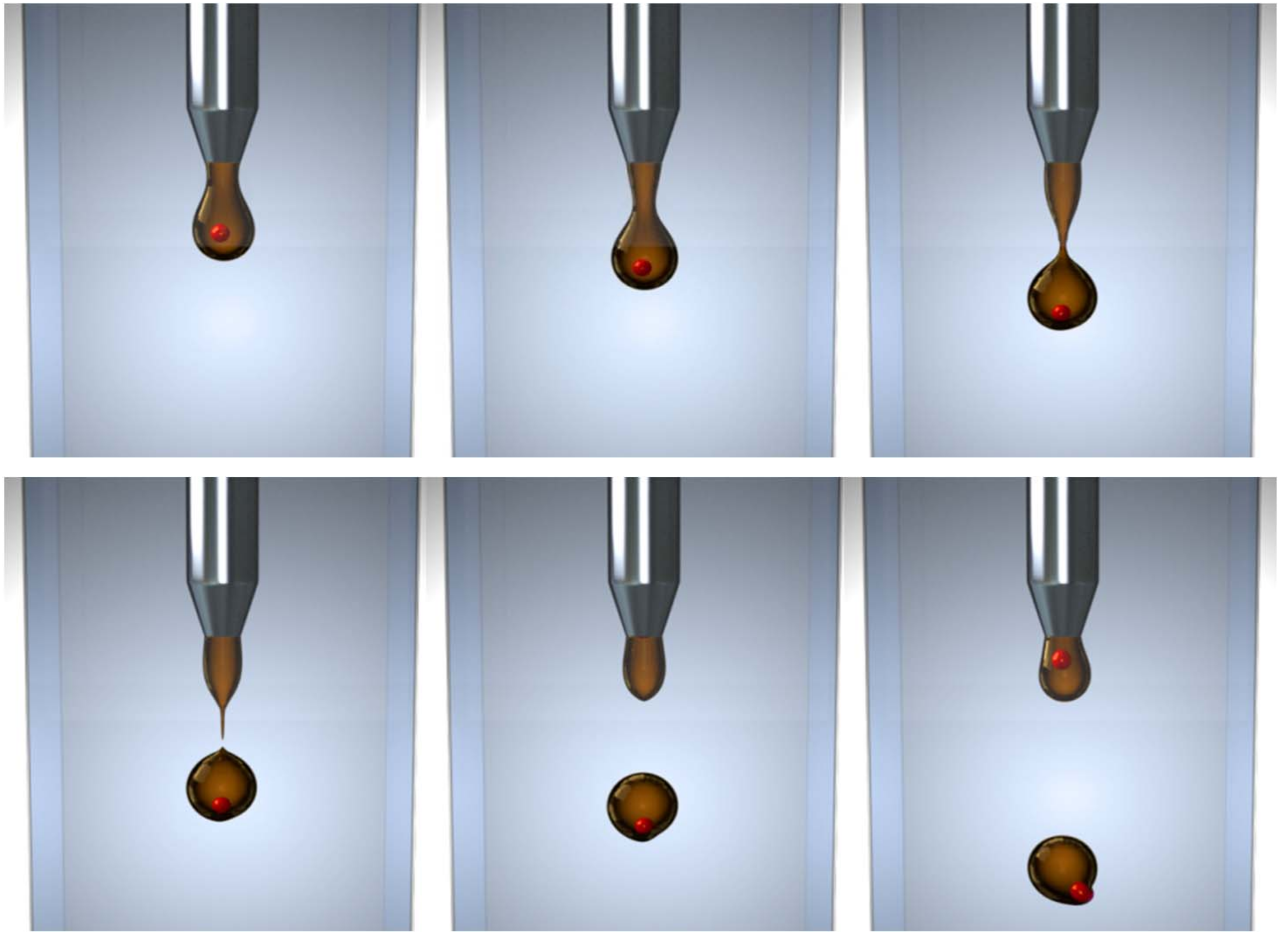

Next Steps

- Adaptive time stepping + adaptive grid alignment/ALE.
- Coupling with turbulence models.
- Coupling with elastic particles, resp., objects (full FSI).
- Integration of 3D viscoelastic multiphase effects into FEM-FBM.
- Benchmarking and experimental validation for „many“ particles/droplets.

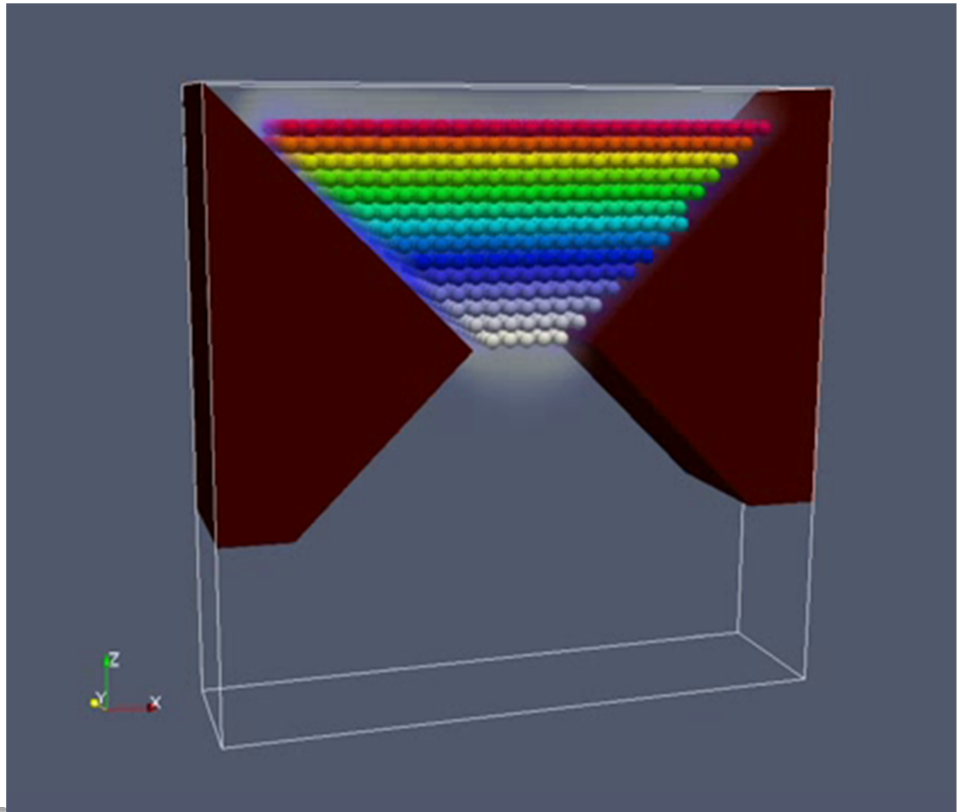

Backup slides …

Benchmarking and Validation

FEM-Multigrid Framework

- *Increasing the mesh resolution produces more accurate results*

  Test performed at different mesh levels
  - Maximum velocity is approximated better ✓
  - Shape of the velocity curve matches better ✓

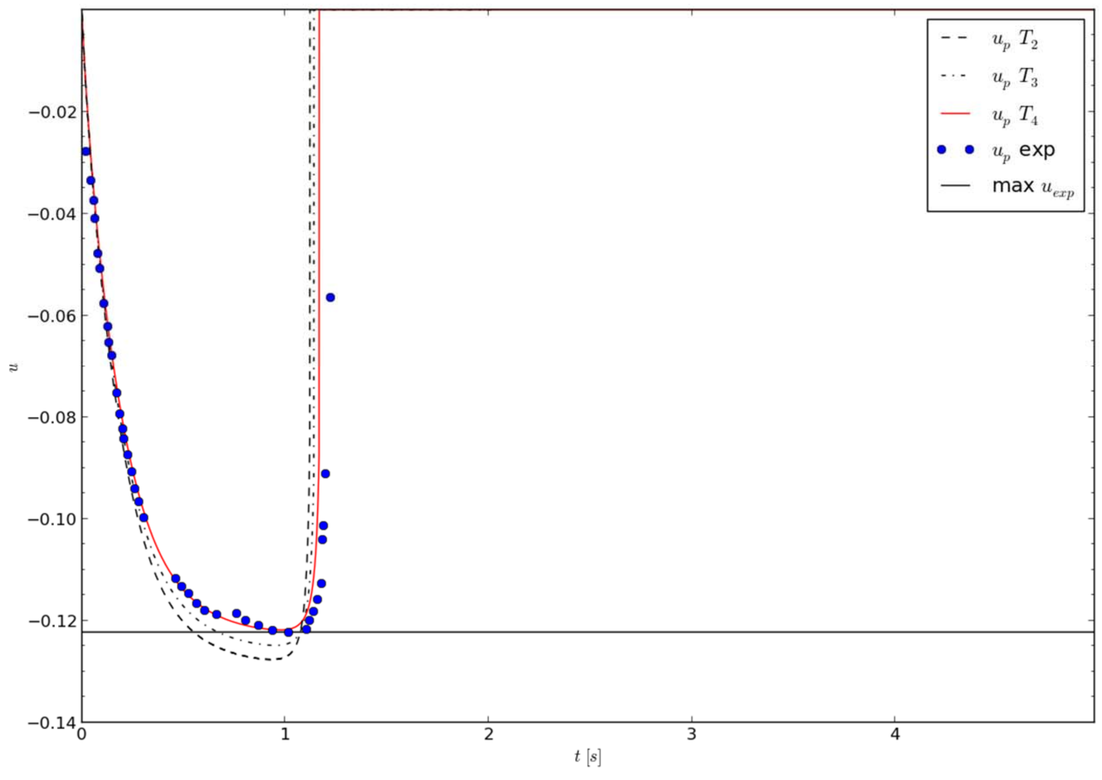

Preliminary Numerical Results – 3D Three-phase Flow

Rise of a light droplet carrying an entrapped particle in a surrounding heavier liquid

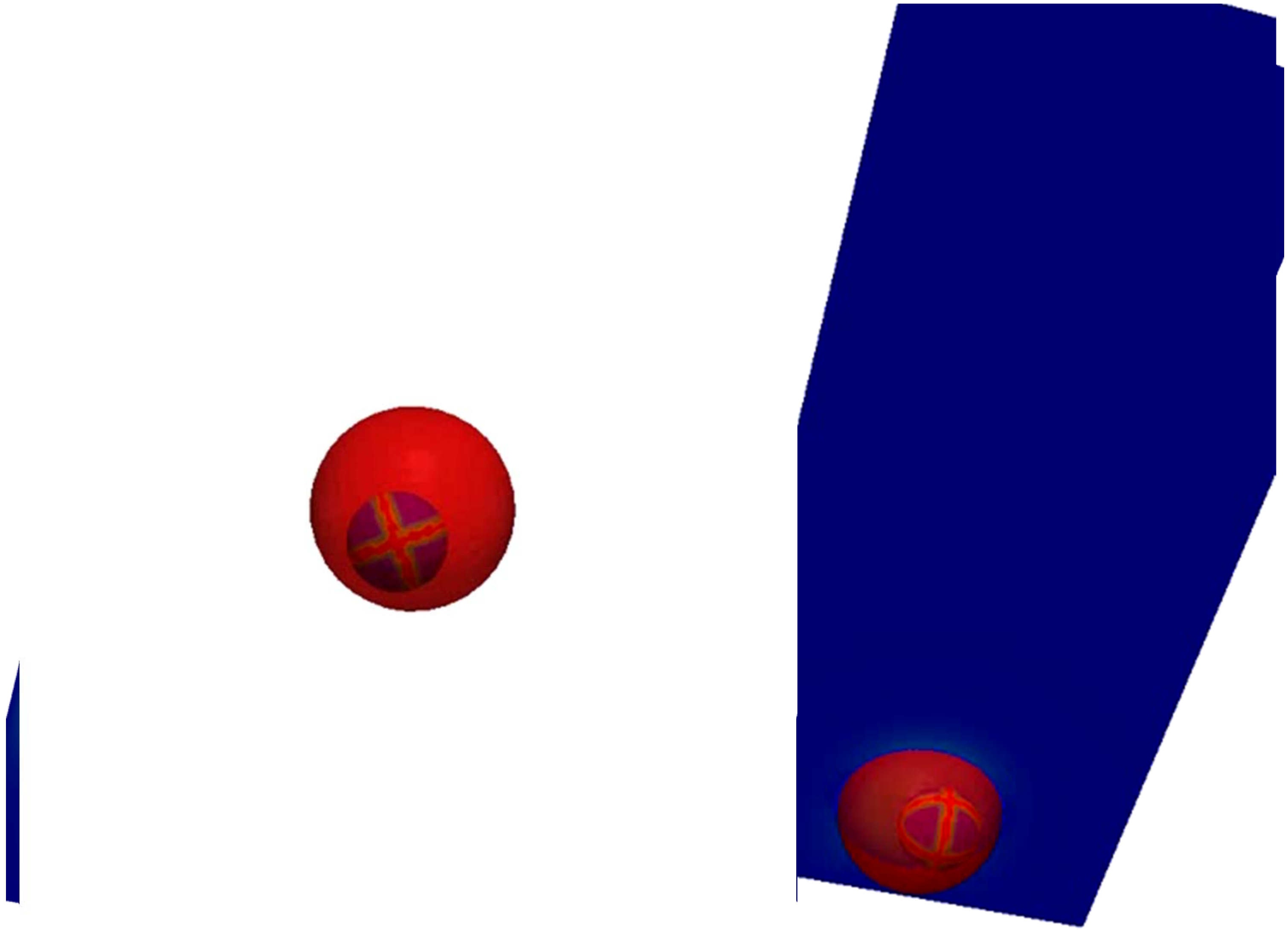

Benchmarking and Validation

Free fall of particles:

- Terminal velocity
- Different physical parameters
- Different geometrical parameters

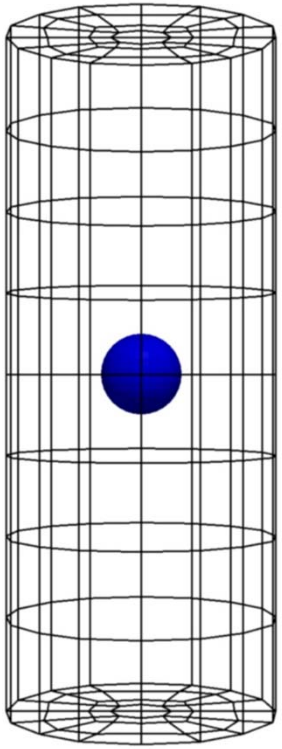

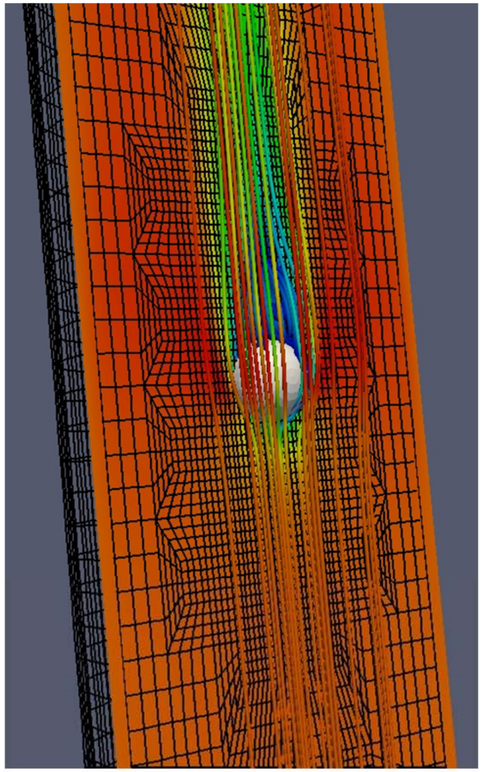

Münster, R.; Mierka, O.; Turek, S.: Finite Element fictitious boundary methods (FEM-FBM) for 3D particulate flow, IJNMF, 2010, accepted

$d_s = 0.3, \quad \rho_s = 1.14$

ν	$U_{featflow}$	U_{exp}	Relative error (%)
0.02	5.885	6.283	6.33
0.05	4.133	3.972	4.05
0.1	2.588	2.426	6.66
0.2	1.492	1.401	6.50

$d_s = 0.2, \quad \rho_s = 1.14$

ν	$U_{featflow}$	U_{exp}	Relative error (%)
0.02	4.370	4.334	0.83
0.05	2.699	2.489	8.44
0.1	1.649	1.552	6.25
0.2	0.946	0.870	8.74

$d_s = 0.3, \quad \rho_s = 1.02$

ν	$U_{featflow}$	U_{exp}	Relative error (%)
0.01	2.167	2.107	2.84
0.02	1.495	1.436	4.11
0.05	0.809	0.749	8.01
0.1	0.402	0.404	0.44
0.2	0.218	0.216	1.02

$d_s = 0.2, \quad \rho_s = 1.02$

ν	$U_{featflow}$	U_{exp}	Relative error (%)
0.01	1.4660	1.4110	3.90
0.02	0.9998	0.9129	9.52
0.05	0.4917	0.4603	6.82
0.1	0.2637	0.2571	2.57
0.2	0.1335	0.1317	1.37

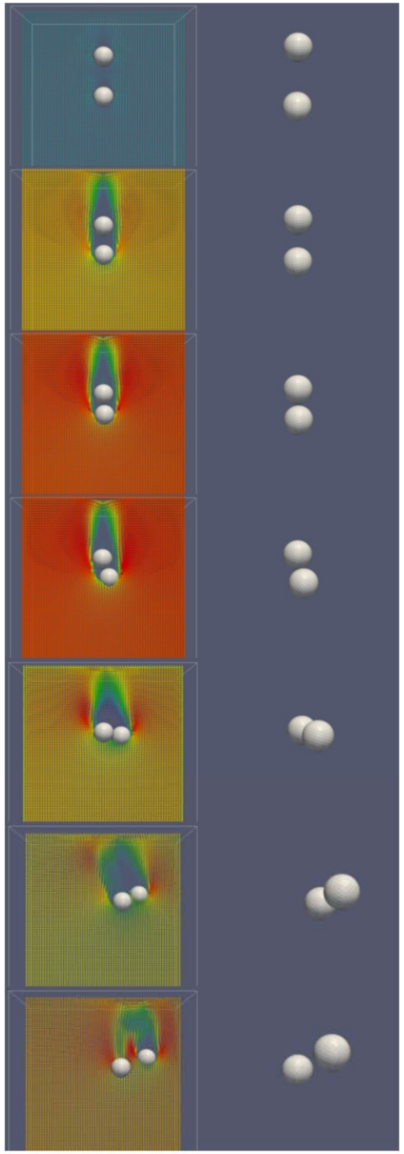

3D Simulations with more Complex Geometries

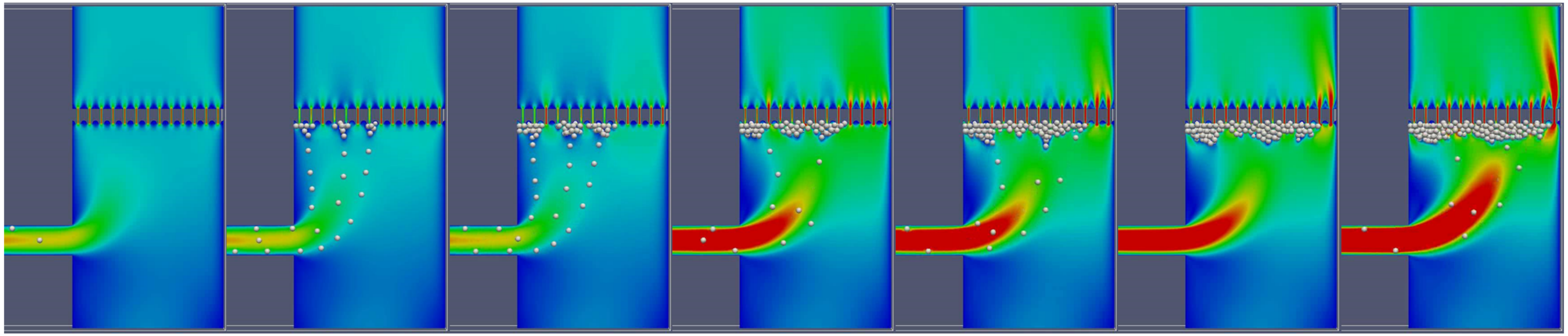

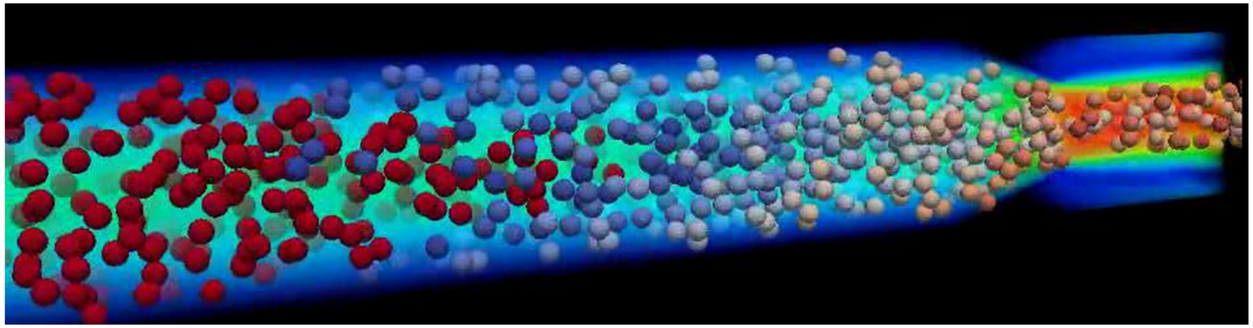

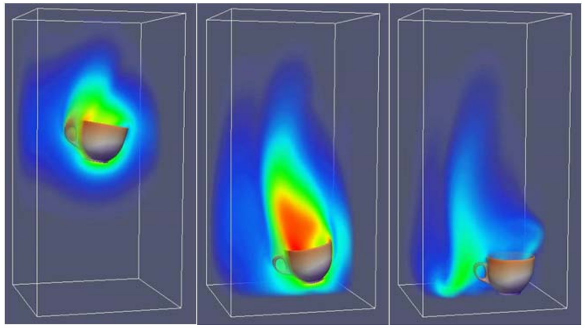

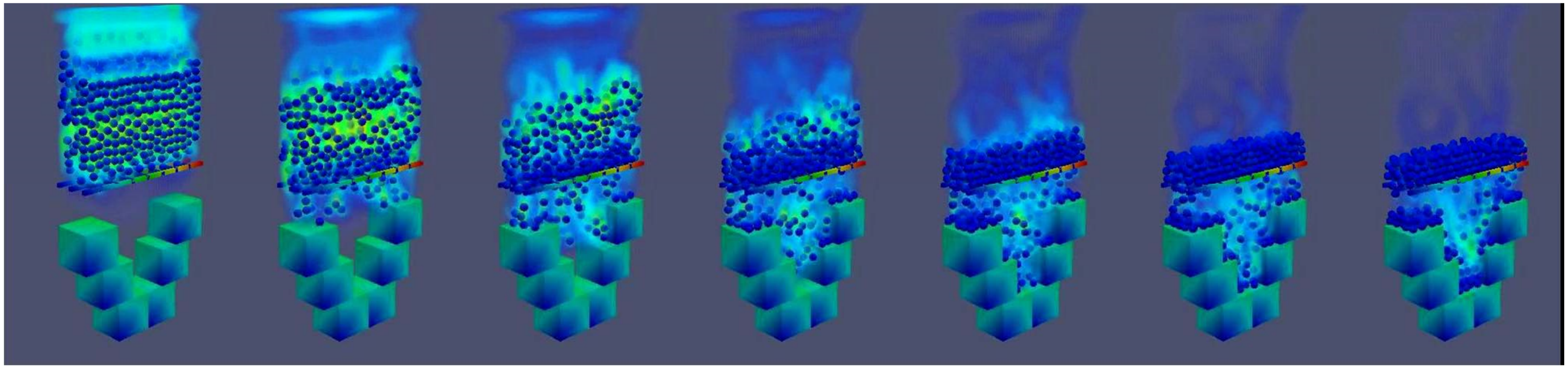

Numerical Benchmarking

2D Bubble Benchmarks

http://www.featflow.de/beta/en/benchmarks/

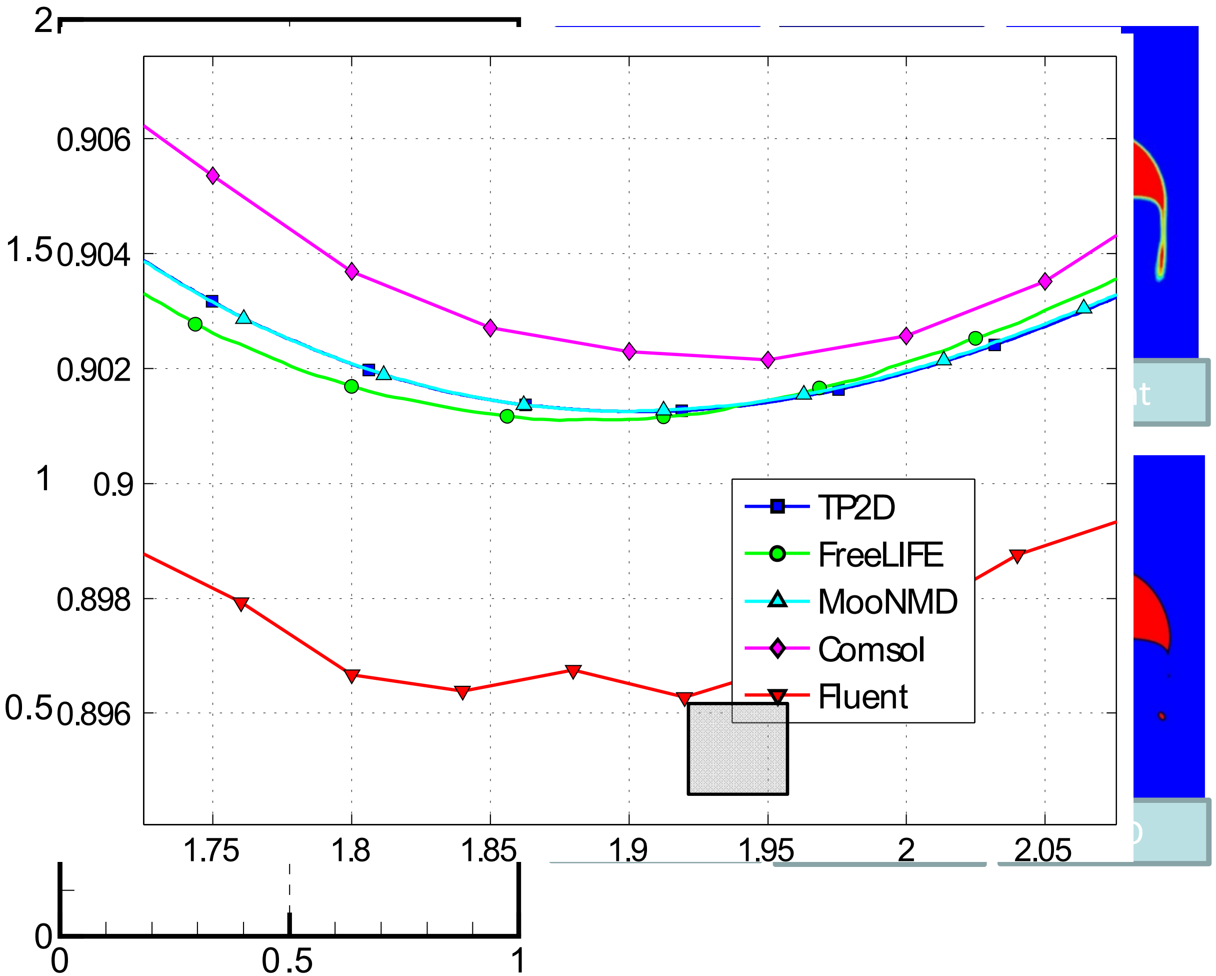

Benchmark quantities

Center of mass	$\mathbf{x}_c = \dfrac{\int_{\Omega_2} \mathbf{x}\, dx}{\int_{\Omega_2} 1\, dx}$
Mean rise velocity	$\mathbf{U}_c = \dfrac{\int_{\Omega_2} \mathbf{u}\, dx}{\int_{\Omega_2} 1\, dx}$
Circularity	$¢ = \dfrac{P_a}{P_b} = \dfrac{\pi d_a}{P_b}$

Hysing, S.; Turek, S.; Kuzmin, D.; Parolini, N.; Burman, E.; Ganesan, S.; Tobiska, L.:
Quantitative benchmark computations of two-dimensional bubble dynamics,
International Journal for Numerical Methods in Fluids, 2009

Aim: Tailored Monodisperse Droplets via Modulation

In case of monodisperse droplet generation:

$$\dot{V}_D = f V_{\mathrm{droplet}}$$

Influencable variables

On the level of the process:

- Flow rates
- Modulation frequency
- Modulation amplitude

Geometrical changes:

- Capillary size
- Contraction angle
- Contraction ratio

No Regulation
Flowrate: 100%
Capillary: STD
Droplet size: 5.2mm

Regulated
Flowrate: 100%
Capillary: STD
Droplet size: 5.0mm

Regulated
Flowrate: 150%
Capillary: STD
Droplet size: 5.7mm

Regulated
Flowrate: 75%
Capillary: STD
Droplet size: 4.5mm

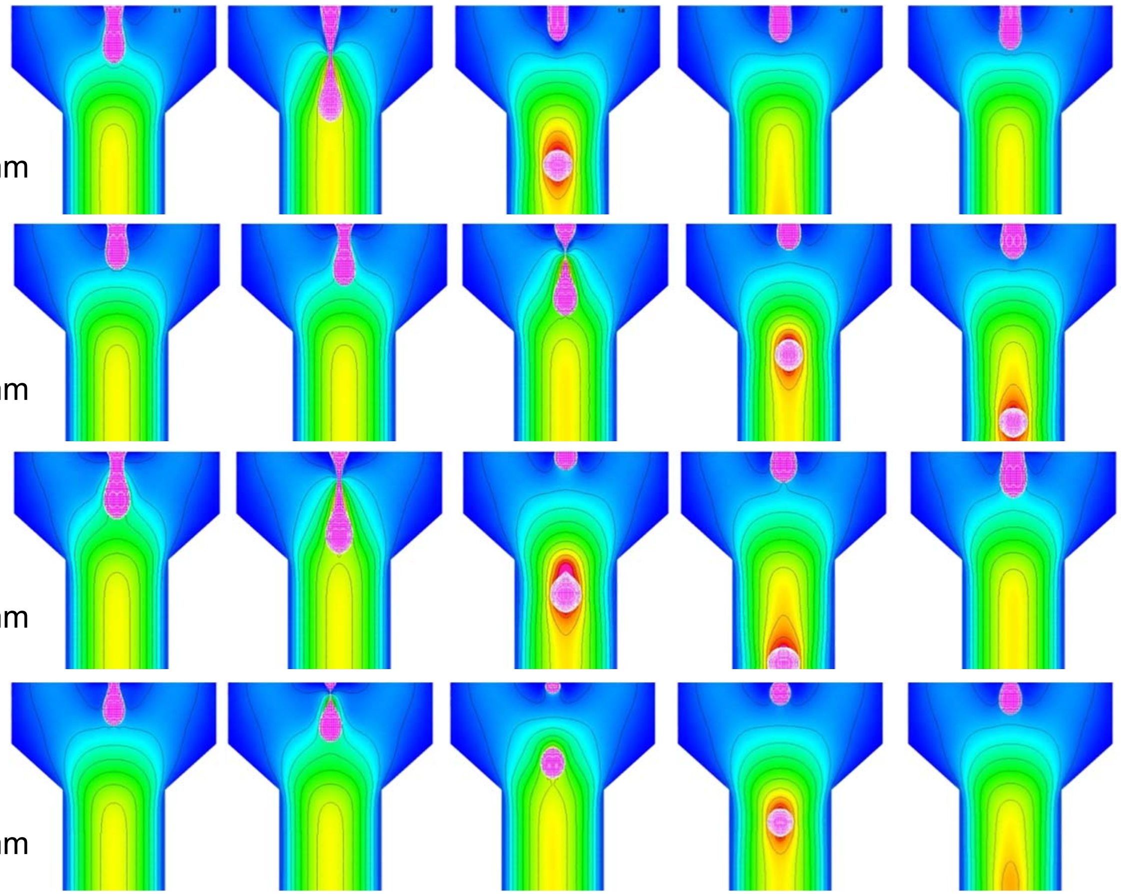

Modulation function

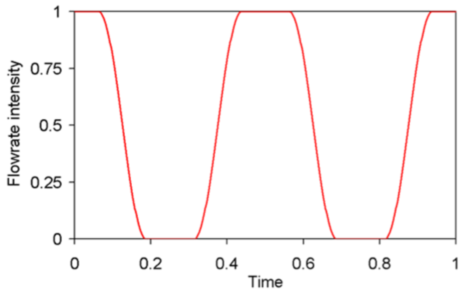

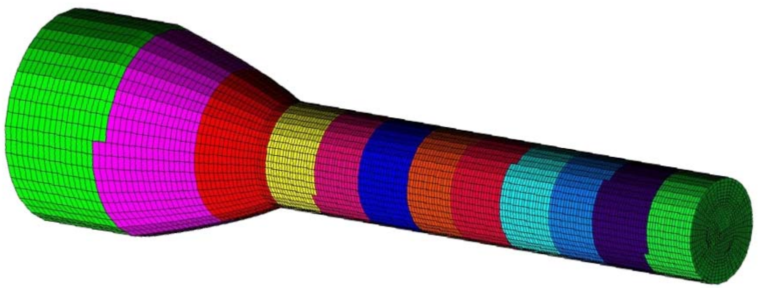

Resulting operation envelope:

- Size: 4.5 mm – 5.7 mm
- Volume: 0.38 cm^3 – 0.77 cm^3

DGS Configuration